

See discussions, stats, and author profiles for this publication at: <https://www.researchgate.net/publication/359119115>

Design, synthesis, and in vitro and in vivo anticancer activity studies of new (S)-Naproxen thiosemicarbazide/1,2,4-triazole derivatives

Article in *New Journal of Chemistry* · January 2022

DOI: 10.1039/D1NJ05899A

CITATIONS

10

READS

370

9 authors, including:



Ihsan Han
Erciyes University

29 PUBLICATIONS 460 CITATIONS

SEE PROFILE



Cansu Ümran Tunç
University of Utah

16 PUBLICATIONS 175 CITATIONS

SEE PROFILE



Ömer ERDOĞAN
Gaziantep Islam Science and Technology University

76 PUBLICATIONS 621 CITATIONS

SEE PROFILE



Ş.Güniz Küçükgülzel
Fenerbahçe University

98 PUBLICATIONS 5,623 CITATIONS

SEE PROFILE

PAPER



Cite this: *New J. Chem.*, 2022, 46, 6046

Design, synthesis, and *in vitro* and *in vivo* anticancer activity studies of new (S)-Naproxen thiosemicarbazide/1,2,4-triazole derivatives†

M.İhsan Han,^{id}*^a Cansu Ümran Tunç,^{bcd} Pınar Atalay,^{be} Ömer Erdoğan,^f Gökhan Ünal,^{cgh} Mehmet Bozkurt,^{cgh} Ömer Aydın,^{id}^{cdij} Özge Çevik^f and Ş. Güniz Küçükgülzel^k

In this study, a series of novel (S)-Naproxen derivatives bearing a thiosemicarbazide/1,2,4-triazole moiety were designed, synthesized, and evaluated for anticancer activity. The structures of these compounds were characterized by spectral (¹H-¹³C NMR, FT-IR, and HR-MS analyses) methods. All of the synthesized compounds (**3a–m**, **4a–j**) were screened for anticancer activity against human breast cancer cell line MDA-MB-231. Among them, (S)-4-(2,4-dichlorophenyl)-5-[1-(6-methoxynaphthalen-2-yl)ethyl]-4H-1,2,4-triazole-3-thione (**4b**) showed the most potent anticancer activity with a good selectivity (IC₅₀ = 9.89 ± 2.4 μM). Inhibition of anti-apoptotic protein Bcl-2 was investigated in MDA-MB-231 cells treated with compound **4b** using Western Blotting. Apoptosis was also detected by AO/EB and JC-1 staining. Furthermore, activation of caspase-3 enzyme activity demonstrated apoptosis. The flow cytometric analysis results showed that compound **4b** decreases the number of cells in the G2/M phase and increases the cells in the S phase in a dose-dependent manner. The anticancer activity of compound **4b** was also investigated. In the Ehrlich acid tumor model, a well-validated *in vivo* ectopic breast cancer model, compound **4b** had anticancer activity and reduced the tumor volume at both low (60 mg kg⁻¹) and high (120 mg kg⁻¹) doses in mice, according to our *in vivo* results.

Received 11th December 2021,
Accepted 16th February 2022

DOI: 10.1039/d1nj05899a

rscl.njc

Introduction

Cancer is the uncontrolled growth of abnormal cells in the body. There are more than 100 types of cancer, including breast

cancer. Breast cancer is one of the main reasons for morbidity and mortality in women.¹ It has been a major public health problem in Western countries for many years. Numerous studies of its epidemiology have been undertaken.² There are many factors causing breast cancer, including family history, age, and hormonal factors.³ Different treatment strategies have been applied based on the type of breast cancer.⁴ Triple-negative breast cancer (TNBC) is characterized by the lack of HER2 protein overexpression and the absence of protein expression of the estrogen receptor (ER) and progesterone receptor (PR), and is one of the most difficult types of cancer to treat.⁵ Numerous molecules have been investigated for the treatment of TNBC by researchers.

Naproxen is an active ingredient that reduces inflammation and pain, especially in joints and muscles. It is used in many diseases such as rheumatoid arthritis, osteoarthritis, and gout. Naproxen is actually on prescription as pharmaceutical formulations as a gel or tablet.^{6,7} In the treatment of acute postoperative pain, a single oral dose of naproxen sodium is an efficient analgesic.⁸ In recent years, many researchers have studied the anticancer activity of Naproxen and its derivatives.^{9–25} Molecules containing a thiosemicarbazide structure are intermediate structures used in the synthesis of heterocyclic rings and are also

^a Department of Pharmaceutical Chemistry, Faculty of Pharmacy, Erciyes University, 38039, Kayseri, Turkey. E-mail: hanihsan@gmail.com

^b Drug Application and Research Center, Erciyes University, 38039 Kayseri, Turkey

^c Department of Biomedical Engineering, Faculty of Engineering, Erciyes University, 38039, Kayseri, Turkey

^d Genom and Stem Cell Center, Erciyes University, 38039, Kayseri, Turkey

^e Department of Basic Sciences, Faculty of Pharmacy, Erciyes University, 38039, Kayseri, Turkey

^f Department of Biochemistry, Faculty of Medicine, Aydın Adnan Menderes University, 09100, Aydın, Turkey

^g Department of Pharmacology, Faculty of Pharmacy, Erciyes University, 38039, Kayseri, Turkey

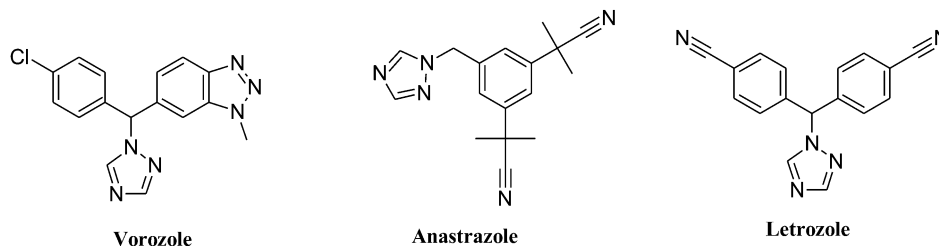
^h DEKAM – Experimental Research and Application Center, Erciyes University, 38039, Kayseri, Turkey

ⁱ ERKAM – Clinical Engineering Research and Application Center, Erciyes University, 38039, Kayseri, Turkey

^j ERNAM – Nanotechnology Research and Application Center, Erciyes University, 38039, Kayseri, Turkey

^k Department of Pharmaceutical Chemistry, Faculty of Pharmacy, Fenerbahçe University, Istanbul, 34758, Istanbul, Turkey

† Electronic supplementary information (ESI) available. See DOI: 10.1039/d1nj05899a



Scheme 1 Compounds containing a 1,2,4-triazole structure with anticancer effects.

bioactive structures. They attract the attention of researchers because of these properties. They have various pharmacological activities, especially anticancer activity.^{25–35} The 1,2,4-triazole ring is a five-membered heterocyclic ring that includes two carbon and three nitrogen atoms. The 1,2,4-triazole ring is synthesized by heating thiosemicarbazides in a basic medium. Structures containing a 1,2,4-triazole ring have anticancer activity.^{36–46} There exist a few molecules with a 1,2,4-triazole ring used in breast cancer, such as Vorozole, Anastrozole, and Letrozole (Scheme 1).^{47,48}

In this study, we synthesized novel (*S*)-Naproxen thiosemicarbazide (**3a–m**) and 1,2,4-triazole derivatives (**4a–j**) and investigated their anticancer activity against breast cancer cell line MDA-MB-231. The characterization of these compounds was identified with FT-IR, ¹H-NMR, ¹³C-NMR, and HR-MS spectral data. The anticancer activity of compound 4b was determined as the strongest compound. In our study, apoptosis assays were expressed by AO/EB and JC-1 staining, inhibition of caspase activity and Bcl-2 expression. Also, suppression of the tumor volume detected for a compound indicates anticancer activity for that compound.

Experimental

Chemistry

Material and methods. All chemicals and solvents were purchased from Sigma Aldrich and Merck. Melting points were taken on Schmelzpunktbestimmer 9300 SMP II apparatus and are uncorrected. Synthesis of these compounds was carried out in the Memmert WNB14 instrument and Heidolph MR Plug Radley. Merck silica gel 60 F254 plates were used for analytical TLC. The purity of the compounds was controlled on TLC plates precoated with silica gel G in a solvent system comprising a petroleum ether:ethyl acetate (40:60 v/v *t*: 25 °C) mixture as an eluent. The spots were located under UV light (254 nm). ¹H-(400 MHz) and ¹³C NMR spectra (100 MHz) were obtained on a BRUKER AM 400 spectrometer in (*d*₆) DMSO solution at the Erciyes University Technology Research and Application Center (TAUM). MS spectra were carried out on an LC/MS High-Resolution Time of Flight (Q-TOF) Agilent 1200/6530 instrument at the Atatürk University-East Anatolian High Technology Research and Application Center (DAYTAM).

Preparation of the (*S*)-Naproxen ester (**1**) and hydrazide (**2**)

These (*S*)-naproxen compounds were prepared according to our literature procedure.^{42,43}

General procedure for the synthesis of (*S*)-*N*-(substituted phenyl/propyl)-2-[2-(6-methoxynaphthalen-2-yl)propanoyl]hydrazine-1-carbothioamide (3a–m**).** Compound **2** (0.01 mol) and substituted isothiocyanate (0.011 mol) were refluxed for 24 h in 20 mL of *n*-butanol. At the end of the reaction, *n*-butanol was evaporated and washed with cold methanol. The solid compound was filtered, washed with water, dried, and recrystallized with ethanol.

***N*-(3-Fluorophenyl)-2-[2-(6-methoxynaphthalen-2-yl)propanoyl]hydrazine-1-carbothioamide (**3a**).** White solid, yield 83%, m.p. 163 °C, *R*_f 0.92; FT-IR ν_{\max} (cm⁻¹): 3129 (N–H), 2959 (Arom. C–H), 2837 (Aliph. C–H), 1671 (C=O), 1544, 1501, 1485, 1453 (Arom. C=C, N–H, C–N), 1262 (C=S), 1216 (C–O), 1161 (C–F). ¹H-NMR (400 MHz, DMSO-*d*₆) δ 1.48 (d, 3H, CH–CH₃), 3.86 (s, 3H, O–CH₃), 4.63 (q, 1H, CH–CH₃), 7.13–7.79 (m, 10H, Ar–H), 9.59 (s, 1H, –CS–NH–), 9.74 (s, 1H, –CO–NH–NH–), 10.17 (s, 1H, –CO–NH–); ¹³C-NMR (100 MHz, DMSO-*d*₆) δ 188.13 (C=S), 173.48 (C=O), 160.79 (C13), 157.55 (C1), 141.32 (C6), 136.96 (C11), 133.71 (C9), 130.03 (C3), 129.55 (C15), 128.85 (C4), 127.08 (C8), 126.32 (C5), 126.07 (C7), 119.25 (C16), 119.05 (C2), 113.36 (C12), 111.52 (C14), 106.22 (C10), 55.62 (CH₃), 40.67 (CH), 19.01 (CH₃); HR-MS (ESI): *m/z* calcd for C₂₁H₂₀FN₃O₂S (M + H)⁺, 398.1333; found 398.1337.

***N*-(2,6-Difluorophenyl)-2-[2-(6-methoxynaphthalen-2-yl)propanoyl]hydrazine-1-carbothioamide (**3b**).** White solid, yield 77%, m.p. 176 °C, *R*_f 0.53; FT-IR ν_{\max} (cm⁻¹): 3170 (N–H), 2992 (Arom. C–H), 2950 (Aliph. C–H), 1685 (C=O), 1578, 1532, 1504, 1471 (Arom. C=C, N–H, C–N), 1268 (C=S), 1237 (C–O), 1119 (C–F). ¹H-NMR (400 MHz, DMSO-*d*₆) δ 1.48 (d, 3H, CH–CH₃), 3.84 (s, 3H, O–CH₃), 4.62 (q, 1H, CH–CH₃), 7.11–7.78 (m, 9H, Ar–H), 9.22 (s, 1H, –CS–NH–), 9.87 (s, 1H, –CO–NH–NH–), 10.24 (s, 1H, –CO–NH–); ¹³C-NMR (100 MHz, DMSO-*d*₆) δ 183.23 (C=S), 175.05 (C=O), 160.63 (C16), 160.54 (C12), 157.51 (C1), 136.96 (C6), 133.68 (C9), 129.55 (C3), 128.83 (C4), 127.14 (C8), 127.02 (C5), 126.11 (C7), 124.85 (C14), 123.00 (C11), 119.00 (C2), 112.25 (C15), 112.02 (C13), 106.19 (C10), 55.62 (CH₃), 43.72 (CH), 18.85 (CH₃); HR-MS (ESI): *m/z* calcd for C₂₁H₁₉F₂N₃O₂S (M + H)⁺, 416.1238; found 416.1244.

***N*-(2,4-Dichlorophenyl)-2-[2-(6-methoxynaphthalen-2-yl)propanoyl]hydrazine-1-carbothioamide (**3c**).** White solid, yield 70%, m.p. 178 °C, *R*_f 0.78; FT-IR ν_{\max} (cm⁻¹): 3180 (N–H), 2963 (Arom. C–H), 2936 (Aliph. C–H), 1671 (C=O), 1524, 1503, 1486, 1459 (Arom. C=C, N–H, C–N), 1261 (C=S), 1213 (C–O), 1088 (C–Cl). ¹H-NMR (400 MHz, DMSO-*d*₆) δ 1.48 (d, 3H, CH–CH₃), 3.86 (s, 3H, O–CH₃), 4.62 (q, 1H, CH–CH₃),

7.13–7.78 (m, 9H, Ar-H), 9.31 (s, 1H, -CS-NH-), 9.85 (s, 1H, -CO-NH-NH-), 10.24 (s, 1H, -CO-NH-); ¹³C-NMR (100 MHz, DMSO-*d*₆) δ 181.36 (C=S), 170.48 (C=O), 157.49 (C1), 139.06 (C6), 134.97 (C11), 133.72 (C9), 130.18 (C14), 129.58 (C13), 129.17 (C3), 128.80 (C4), 127.70 (C15), 127.11 (C8), 126.89 (C5), 126.11 (C7), 122.13 (C12), 119.01 (C16), 118.77 (C2), 106.18 (C10), 55.64 (CH₃), 46.86 (CH), 18.89 (CH₃); HR-MS (ESI): *m/z* calcd for C₂₁H₁₉Cl₂N₃O₂S (M + H)⁺, 448.0647; found 448.0650.

***N*-(2,6-Dichlorophenyl)-2-[2-(6-methoxynaphthalen-2-yl)propanoyl]hydrazine-1-carbothioamide (3d)**. White solid, yield 56%, m.p. 193 °C, *R*_f 0.76; FT-IR ν_{max} (cm⁻¹): 3194 (N-H), 2979 (Arom. C-H), 2961 (Aliph. C-H), 1691 (C=O), 1565, 1507, 1488, 1451 (Arom. C=C, N-H, C-N), 1264 (C=S), 1232 (C-O), 1072 (C-Cl). ¹H-NMR (400 MHz, DMSO-*d*₆) δ 1.48 (d, 3H, CH-CH₃), 3.85 (s, 3H, O-CH₃), 4.64 (q, 1H, CH-CH₃), 7.13–7.77 (m, 9H, Ar-H), 9.42 (s, 1H, -CS-NH-), 9.73 (s, 1H, -CO-NH-NH-), 10.20 (s, 1H, -CO-NH-); ¹³C-NMR (100 MHz, DMSO-*d*₆) δ 182.42 (C=S), 174.00 (C=O), 157.49 (C1), 140.38 (C6), 137.03 (C11), 135.60 (C15), 133.66 (C9), 131.76 (C12), 131.34 (C16), 129.70 (C13), 129.54 (C3), 128.81 (C4), 127.79 (C14), 127.19 (C8), 126.98 (C5), 126.11 (C7), 118.98 (C2), 106.19 (C10), 55.61 (CH₃), 43.77 (CH), 18.94 (CH₃); HR-MS (ESI): *m/z* calcd for C₂₁H₁₉Cl₂N₃O₂S (M + H)⁺, 448.0647; found 448.0653.

***N*-(2-Bromophenyl)-2-[2-(6-methoxynaphthalen-2-yl)propanoyl]hydrazine-1-carbothioamide (3e)**. White solid, yield 23%, m.p. 202 °C, *R*_f 0.76; FT-IR ν_{max} (cm⁻¹): 3169 (N-H), 2966 (Arom. C-H), 2934 (Aliph. C-H), 1669 (C=O), 1575, 1504, 1487, 1459 (Arom. C=C, N-H, C-N), 1259 (C=S), 1213 (C-O), 1048 (C-Br). ¹H-NMR (400 MHz, DMSO-*d*₆) δ 1.48 (d, 3H, CH-CH₃), 3.86 (s, 3H, O-CH₃), 4.51 (q, 1H, CH-CH₃), 7.13–7.78 (m, 10H, Ar-H), 9.26 (s, 1H, -CS-NH-), 9.77 (s, 1H, -CO-NH-NH-), 10.25 (s, 1H, -CO-NH-); ¹³C-NMR (100 MHz, DMSO-*d*₆) δ 178.92 (C=S), 170.63 (C=O), 157.55 (C1), 136.77 (C6), 133.74 (C9), 132.87 (C13), 130.16 (C14), 130.08 (C11), 129.68 (C3), 128.80 (C4), 128.60 (C16), 128.23 (C15), 127.25 (C8), 127.07 (C5), 126.15 (C7), 121.25 (C12), 119.15 (C2), 106.18 (C10), 55.66 (CH₃), 43.74 (CH), 18.82 (CH₃); HR-MS (ESI): *m/z* calcd for C₂₁H₂₀BrN₃O₂S (M + H)⁺, 458.0532; found 458.0536.

***N*-(3-Bromophenyl)-2-[2-(6-methoxynaphthalen-2-yl)propanoyl]hydrazine-1-carbothioamide (3f)**. White solid, yield 17%, m.p. 209 °C, *R*_f 0.73; FT-IR ν_{max} (cm⁻¹): 3135 (N-H), 3009 (Arom. C-H), 2958 (Aliph. C-H), 1673 (C=O), 1571, 1500, 1486, 1459 (Arom. C=C, N-H, C-N), 1265 (C=S), 1216 (C-O), 1029 (C-Br). ¹H-NMR (400 MHz, DMSO-*d*₆) δ 1.48 (d, 3H, CH-CH₃), 3.85 (s, 3H, O-CH₃), 4.58 (q, 1H, CH-CH₃), 7.13–7.79 (m, 10H, Ar-H), 9.57 (s, 1H, -CS-NH-), 9.76 (s, 1H, -CO-NH-NH-), 10.15 (s, 1H, -CO-NH-); ¹³C-NMR (100 MHz, DMSO-*d*₆) δ 181.86 (C=S), 175.22 (C=O), 157.49 (C1), 140.30 (C11), 137.19 (C6), 133.69 (C9), 130.71 (C15), 129.67 (C3), 128.83 (C4), 128.19 (C14), 127.37 (C8), 127.00 (C5), 126.12 (C7), 123.90 (C12), 122.06 (C13), 119.14 (C2), 118.71 (C16), 106.14 (C10), 55.59 (CH₃), 43.75 (CH), 18.57 (CH₃); HR-MS (ESI): *m/z* calcd for C₂₁H₂₀BrN₃O₂S (M + H)⁺, 458.0532; found 458.0550.

***N*-(4-Ethylphenyl)-2-[2-(6-methoxynaphthalen-2-yl)propanoyl]hydrazine-1-carbothioamide (3g)**. White solid, yield 49%, m.p. 161 °C, *R*_f 0.75; FT-IR ν_{max} (cm⁻¹): 3156 (N-H), 2964 (Arom. C-H),

2939 (Aliph. C-H), 1693 (C=O), 1541, 1503, 1479, 1460 (Arom. C=C, N-H, C-N), 1259 (C=S), 1214 (C-O). ¹H-NMR (400 MHz, DMSO-*d*₆) δ 1.17 (t, 3H, CH₂-CH₃), 1.48 (d, 3H, CH-CH₃), 2.57 (q, 1H, CH₂-CH₃), 3.86 (s, 3H, O-CH₃), 4.55 (q, 1H, CH-CH₃), 7.13–7.78 (m, 10H, Ar-H), 9.40 (s, 1H, -CS-NH-), 9.50 (s, 1H, -CO-NH-NH-), 10.10 (s, 1H, -CO-NH-); ¹³C-NMR (100 MHz, DMSO-*d*₆) δ 182.42 (C=S), 173.52 (C=O), 157.52 (C1), 152.66 (C14), 140.96 (C6), 137.12 (C11), 133.69 (C9), 129.56 (C15), 129.40 (C13), 129.27 (C3), 128.84 (C4), 127.86 (C8), 127.09 (C16), 126.35 (C5), 126.05 (C7), 119.05 (C2), 115.85 (C12), 106.17 (C10), 55.62 (CH₃), 43.56 (CH), 28.11 (CH₂), 18.75 (CH₃), 16.07 (CH₃); HR-MS (ESI): *m/z* calcd for C₂₃H₂₅N₃O₂S (M + H)⁺, 408.1740; found 408.1746.

***N*-(4-Nitrophenyl)-2-[2-(6-methoxynaphthalen-2-yl)propanoyl]hydrazine-1-carbothioamide (3h)**. Yellow solid, yield 42%, m.p. 187 °C, *R*_f 0.77; FT-IR ν_{max} (cm⁻¹): 3149 (N-H), 2965 (Arom. C-H), 2940 (Aliph. C-H), 1680 (C=O), 1597, 1571, 1500, 1464, 1415 (Arom. C=C, N-H, C-N, N-O), 1264 (C=S), 1215 (C-O). ¹H-NMR (400 MHz, DMSO-*d*₆) δ 1.48 (d, 3H, CH-CH₃), 3.86 (s, 3H, O-CH₃), 4.55 (q, 1H, CH-CH₃), 7.14–8.20 (m, 10H, Ar-H), 9.26 (s, 1H, -CS-NH-), 9.87 (s, 1H, -CO-NH-NH-), 10.20 (s, 1H, -CO-NH-); ¹³C-NMR (100 MHz, DMSO-*d*₆) δ 182.67 (C=S), 176.77 (C=O), 157.54 (C1), 140.29 (C14), 140.14 (C6), 136.84 (C11), 133.71 (C9), 129.57 (C3), 128.82 (C4), 128.56 (C15), 127.21 (C13), 127.07 (C8), 126.08 (C5), 124.63 (C7), 119.08 (C2), 114.05 (C16), 113.80 (C12), 106.17 (C10), 55.62 (CH₃), 43.72 (CH), 18.79 (CH₃); HR-MS (ESI): *m/z* calcd for C₂₁H₂₀N₄O₄S (M + H)⁺, 425.1278; found 425.1285.

***N*-(3-Pyridil)-2-[2-(6-methoxynaphthalen-2-yl)propanoyl]hydrazine-1-carbothioamide (3i)**. Yellow solid, yield 57%, m.p. 173 °C, *R*_f 0.35; FT-IR ν_{max} (cm⁻¹): 3125 (N-H), 2959 (Arom. C-H), 2936 (Aliph. C-H), 1663 (C=O), 1634 (C=N), 1526, 1503, 1481, 1446 (Arom. C=C, N-H, C-N), 1253 (C=S), 1225 (C-O). ¹H-NMR (400 MHz, DMSO-*d*₆) δ 1.48 (d, 3H, CH-CH₃), 3.86 (s, 3H, O-CH₃), 4.57 (q, 1H, CH-CH₃), 7.13–7.79 (m, 10H, Ar-H), 9.23 (s, 1H, -CS-NH-), 9.81 (s, 1H, -CO-NH-NH-), 10.20 (s, 1H, -CO-NH-); ¹³C-NMR (100 MHz, DMSO-*d*₆) δ 180.44 (C=S), 173.81 (C=O), 157.48 (C1), 146.79 (C13), 137.29 (C6), 136.76 (C11), 136.33 (C12), 133.68 (C9), 129.59 (C3), 128.76 (C4), 127.24 (C8), 126.81 (C5), 126.03 (C7), 123.74 (C14), 119.10 (C2), 113.97 (C15), 106.09 (C10), 55.59 (CH₃), 43.66 (CH), 18.69 (CH₃); HR-MS (ESI): *m/z* calcd for C₂₁H₂₀N₄O₄S (M + H)⁺, 381.1379; found 381.1382.

***N*-(Propyl)-2-[2-(6-methoxynaphthalen-2-yl)propanoyl]hydrazine-1-carbothioamide (3j)**. White solid, yield 55%, m.p. 165 °C, *R*_f 0.60; FT-IR ν_{max} (cm⁻¹): 3167 (N-H), 3008 (Arom. C-H), 2958 (Aliph. C-H), 1668 (C=O), 1549, 1503, 1485, 1459 (Arom. C=C, N-H, C-N), 1261 (C=S), 1216 (C-O). ¹H-NMR (400 MHz, DMSO-*d*₆) δ 0.75 (t, 3H, CH₂-CH₂-CH₃), 0.86 (m, 2H, CH₂-CH₂-CH₃), 1.45 (d, 3H, CH-CH₃), 2.50 (t, 2H, CH₂-CH₂-CH₃), 3.85 (s, 3H, O-CH₃), 4.63 (q, 1H, CH-CH₃), 7.13–7.78 (m, 6H, Ar-H), 9.15 (s, 1H, -CS-NH-), 9.50 (s, 1H, -CO-NH-NH-), 9.91 (s, 1H, -CO-NH-); ¹³C-NMR (100 MHz, DMSO-*d*₆) δ 181.80 (C=S), 174.08 (C=O), 157.49 (C1), 136.82 (C6), 133.69 (C9), 129.59 (C3), 128.77 (C4), 127.30 (C8), 126.80 (C5), 125.91 (C7), 119.11 (C2), 106.07 (C10), 55.59 (CH₃), 45.75 (CH₂), 43.58 (CH), 22.15 (CH₂),

18.40 (CH₃), 11.36 (CH₃); HR-MS (ESI): *m/z* calcd for C₁₈H₂₃N₃O₂S (M + H)⁺, 346.1583; found 346.1584.

N-(Cyclohexylmethyl)-2-[2-(6-methoxynaphthalen-2-yl)propanoyl]hydrazine-1-carbothioamide (3k). White solid, yield 31%, m.p. 192 °C, *R_f* 0.70; FT-IR ν_{\max} (cm⁻¹): 3174 (N-H), 2972 (Arom. C-H), 2924 (Aliph. C-H), 1686 (C=O), 1548, 1505, 1486, 1447 (Arom. C=C, N-H, C-N), 1265 (C=S), 1214 (C-O). ¹H-NMR (400 MHz, DMSO-*d*₆) δ 0.75–1.04 (m, 11H, CH, -CH₂-), 1.45 (d, 3H, CH-CH₃), 2.50 (t, 2H, -CH₂-), 3.85 (s, 3H, O-CH₃), 4.62 (q, 1H, CH-CH₃), 7.13–7.79 (m, 6H, Ar-H), 9.16 (s, 1H, -CS-NH-), 9.48 (s, 1H, -CO-NH-NH-), 9.93 (s, 1H, -CO-NH-); ¹³C-NMR (100 MHz, DMSO-*d*₆) δ 181.89 (C=S), 173.96 (C=O), 157.53 (C1), 136.84 (C6), 133.73 (C9), 129.60 (C3), 128.81 (C4), 127.34 (C8), 126.69 (C5), 125.88 (C7), 119.13 (C2), 106.11 (C10), 55.60 (CH₃), 50.11 (CH₂), 43.58 (CH), 37.14 (CH), 30.46 (CH₂), 30.38 (CH₂), 26.34 (CH₂), 25.65 (CH₂), 22.35 (CH₂), 18.27 (CH₃); HR-MS (ESI): *m/z* calcd for C₂₂H₂₉N₃O₂S (M + H)⁺, 400.2053; found 400.2058.

N-(Benzyl)-2-[2-(6-methoxynaphthalen-2-yl)propanoyl]hydrazine-1-carbothioamide (3l). White solid, yield 31%, m.p. 153 °C, *R_f* 0.75; FT-IR ν_{\max} (cm⁻¹): 3159 (N-H), 2958 (Arom. C-H), 2928 (Aliph. C-H), 1686 (C=O), 1553, 1504, 1483, 1454 (Arom. C=C, N-H, C-N), 1263 (C=S), 1214 (C-O). ¹H-NMR (400 MHz, DMSO-*d*₆) δ 1.45 (d, 3H, CH-CH₃), 3.34 (s, 2H, -CH₂-), 3.86 (s, 3H, O-CH₃), 4.72 (q, 1H, CH-CH₃), 7.15–7.76 (m, 11H, Ar-H), 9.20 (s, 1H, -CS-NH-), 9.33 (s, 1H, -CO-NH-NH-), 10.00 (s, 1H, -CO-NH-); ¹³C-NMR (100 MHz, DMSO-*d*₆) δ 183.20 (C=S), 172.14 (C=O), 157.47 (C1), 139.29 (C11), 136.84 (C6), 133.65 (C9), 129.59 (C3), 128.75 (C14), 128.58 (C4), 128.16 (C15), 128.13 (C13), 127.64 (C12), 127.61 (C16), 127.23 (C8), 126.88 (C5), 125.96 (C7), 119.08 (C2), 106.08 (C10), 55.59 (CH₃), 47.08 (CH₂), 43.64 (CH), 18.64 (CH₃); HR-MS (ESI): *m/z* calcd for C₂₂H₂₃N₃O₂S (M + H)⁺, 394.1583; found 394.1592.

N-(Benzoyl)-2-[2-(6-methoxynaphthalen-2-yl)propanoyl]hydrazine-1-carbothioamide (3m). Grey solid, yield 28%, m.p. 145 °C, *R_f* 0.90; FT-IR ν_{\max} (cm⁻¹): 3151 (N-H), 2975 (Arom. C-H), 2932 (Aliph. C-H), 1653 (C=O), 1547, 1506, 1454, 1424 (Arom. C=C, N-H, C-N), 1260 (C=S), 1213 (C-O). ¹H-NMR (400 MHz, DMSO-*d*₆) δ 1.49 (d, 3H, CH-CH₃), 3.86 (s, 3H, O-CH₃), 4.07 (q, 1H, CH-CH₃), 7.13–7.94 (m, 11H, Ar-H), 11.11 (s, 1H, -CS-NH-), 11.68 (s, 1H, -CO-NH-NH-), 12.67 (s, 1H, -CO-NH-); ¹³C-NMR (100 MHz, DMSO-*d*₆) δ 177.23 (C=S), 171.13 (C=O), 168.43 (C=O), 157.57 (C1), 136.56 (C6), 133.73 (C9), 133.57 (C11), 129.62 (C14), 129.13 (C3), 128.88 (C4), 128.81 (C13), 127.63 (C16), 127.12 (C8), 127.02 (C12), 126.22 (C7), 126.07 (C5), 125.88 (C15), 119.08 (C2), 106.18 (C10), 55.62 (CH₃), 42.86 (CH), 18.75 (CH₃); HR-MS (ESI): *m/z* calcd for C₂₂H₂₁N₃O₃S (M + H)⁺, 408.1376; found 408.1379.

General procedure for the synthesis of 4-(substitutedphenyl/propyl)-5-[1-(6-methoxynaphthalen-2-yl)ethyl]-4H-1,2,4-triazole-3-thione (4a-j). A solution of many thiosemicarbazide compounds (0.01 mol) was heated under Radley for 24 h, in 4 N sodium hydroxide solution (20 mL). The solution was set to pH 6 by glacial acetic acid after cooling to room temperature. The product was precipitated, filtered and washed with distilled water. The compounds were obtained by recrystallization from ethanol.

4-(3-Fluorophenyl)-5-[1-(6-methoxynaphthalen-2-yl)ethyl]-4H-1,2,4-triazole-3-thione (4a). Beige solid, yield 58%, m.p. 172 °C, *R_f* 0.83; FT-IR ν_{\max} (cm⁻¹): 3149 (N-H), 3034 (Arom. C-H), 2931 (Aliph. C-H), 1632 (C=N), 1565, 1507, 1484, 1448 (Arom. C=C, N-H, C-N), 1264 (C=S), 1228 (C-O), 1108 (C-F). ¹H-NMR (400 MHz, DMSO-*d*₆) δ 1.55 (d, 3H, CH-CH₃), 3.85 (s, 3H, O-CH₃), 4.38 (q, 1H, CH-CH₃), 7.08–7.63 (m, 10H, Ar-H), 8.64 (s, 1H, -NH); ¹³C-NMR (100 MHz, DMSO-*d*₆) δ 168.25 (C=S), 160.89 (C15), 157.58 (C1), 154.85 (C11), 144.97 (C13), 136.32 (C6), 133.55 (C9), 129.46 (C3), 128.59 (C4), 127.58 (C8), 125.92 (C5), 125.88 (C7), 125.03 (C-17), 119.21 (C2), 116.07 (C-18), 110.29 (C16), 106.07 (C10), 104.30 (C14), 55.56 (CH₃), 37.10 (CH), 20.30 (CH₃); HR-MS (ESI): *m/z* calcd for C₂₁H₁₈FN₃OS (M + H)⁺, 380.1227; found 380.1236.

4-(2,4-Dichlorophenyl)-5-[1-(6-methoxynaphthalen-2-yl)ethyl]-4H-1,2,4-triazole-3-thione (4b). White solid, yield 27%, m.p. 323 °C, *R_f* 0.86; FT-IR ν_{\max} (cm⁻¹): 3128 (N-H), 2964 (Arom. C-H), 2924 (Aliph. C-H), 1634 (C=N), 1561, 1501, 1484, 1440 (Arom. C=C, N-H, C-N), 1264 (C=O), 1230 (C-O), 1027 (C-Cl). ¹H-NMR (400 MHz, DMSO-*d*₆) δ 1.60 (d, 3H, CH-CH₃), 3.80 (s, 3H, O-CH₃), 6.43 (q, 1H, CH-CH₃), 6.96–7.60 (m, 9H, Ar-H), 8.61 (s, 1H, -NH); ¹³C-NMR (100 MHz, DMSO-*d*₆) δ 167.89 (C=S), 157.51 (C1), 154.65 (C11), 142.71 (C13), 135.50 (C6), 133.67 (C9), 132.30 (C17), 129.77 (C16), 129.36 (C3), 128.83 (C4), 128.59 (C15), 127.43 (C8), 126.34 (C5), 126.21 (C7), 122.19 (C18), 119.09 (C2), 117.94 (C14), 106.09 (C10), 55.55 (CH₃), 37.14 (CH), 20.02 (CH₃); HR-MS (ESI): *m/z* calcd for C₂₁H₁₇Cl₂N₃OS (M + H)⁺, 430.0542; found 430.0549.

4-(2,6-Dichlorophenyl)-5-[1-(6-methoxynaphthalen-2-yl)ethyl]-4H-1,2,4-triazole-3-thione (4c). White solid, yield 31%, m.p. 236 °C, *R_f* 0.90; FT-IR ν_{\max} (cm⁻¹): 3169 (N-H), 3046 (Arom. C-H), 2932 (Aliph. C-H), 1633 (C=N), 1568, 1503, 1476, 1441 (Arom. C=C, N-H, C-N), 1262 (C=O), 1212 (C-O), 1029 (C-Cl). ¹H-NMR (400 MHz, DMSO-*d*₆) δ 1.60 (d, 3H, CH-CH₃), 3.84 (s, 3H, O-CH₃), 5.32 (q, 1H, CH-CH₃), 7.08–7.63 (m, 9H, Ar-H), 8.68 (s, 1H, -NH); ¹³C-NMR (100 MHz, DMSO-*d*₆) δ 168.03 (C=S), 157.58 (C1), 153.93 (C11), 135.68 (C6), 134.16 (C13), 133.82 (C9), 129.67 (C15), 129.62 (C17), 129.28 (C3), 128.68 (C4), 127.81 (C16), 127.39 (C8), 126.24 (C5), 125.22 (C7), 121.46 (C18), 121.34 (C14), 119.08 (C2), 106.15 (C10), 55.57 (CH₃), 37.70 (CH), 20.50 (CH₃); HR-MS (ESI): *m/z* calcd for C₂₁H₁₇Cl₂N₃OS (M + H)⁺, 430.0542; found 430.0548.

4-(3-Bromophenyl)-5-[1-(6-methoxynaphthalen-2-yl)ethyl]-4H-1,2,4-triazole-3-thione (4d). Grey solid, yield 50%, m.p. 210 °C, *R_f* 0.90; FT-IR ν_{\max} (cm⁻¹): 3170 (N-H), 3046 (Arom. C-H), 2921 (Aliph. C-H), 1643 (C=N), 1566, 1505, 1474, 1426 (Arom. C=C, N-H, C-N), 1264 (C=O), 1229 (C-O), 1030 (C-Br). ¹H-NMR (400 MHz, DMSO-*d*₆) δ 1.54 (d, 3H, CH-CH₃), 3.83 (s, 3H, O-CH₃), 4.04 (q, 1H, CH-CH₃), 7.07–7.64 (m, 10H, Ar-H), 8.65 (s, 1H, -NH); ¹³C-NMR (100 MHz, DMSO-*d*₆) δ 168.38 (C=S), 157.63 (C1), 154.86 (C11), 136.08 (C6), 135.17 (C13), 133.64 (C9), 132.71 (C17), 129.30 (C3), 128.63 (C4), 127.92 (C16), 127.62 (C8), 126.02 (C5), 125.83 (C7), 122.68 (C15), 122.41 (C14), 121.69 (C18), 119.25 (C2), 106.11 (C10), 55.59 (CH₃), 37.19 (CH), 20.16 (CH₃); HR-MS (ESI): *m/z* calcd for C₂₁H₁₈BrN₃OS (M + H)⁺, 440.0426; found 440.0426.

4-(4-Ethylphenyl)-5-[1-(6-methoxynaphthalen-2-yl)ethyl]-4H-1,2,4-triazole-3-thione (4e). Pink solid, yield 30%, m.p. 118 °C, R_f 0.86; FT-IR ν_{\max} (cm⁻¹): 3179 (N-H), 2964 (Arom. C-H), 2923 (Aliph. C-H), 1633 (C=N), 1550, 1515, 1488, 1405 (Arom. C=C, N-H, C-N), 1266 (C=S), 1216 (C-O). ¹H-NMR (400 MHz, DMSO-*d*₆) δ 1.12 (t, 1H, CH₂-CH₃), 1.52 (d, 3H, CH-CH₃), 2.55 (q, 1H, CH₂-CH₃), 3.93 (s, 3H, O-CH₃), 4.32 (q, 1H, CH-CH₃), 7.02-7.62 (m, 10H, Ar-H), 8.59 (s, 1H, -NH); ¹³C-NMR (100 MHz, DMSO-*d*₆) δ 176.22 (C=S), 157.44 (C1), 155.53 (C11), 153.72 (C16), 144.34 (C13), 136.94 (C6), 133.63 (C9), 129.45 (C3), 128.59 (C4), 128.45 (C15), 128.42 (C-17), 127.41 (C8), 126.26 (C7), 126.00 (C5), 119.05 (C2), 113.61 (C-18), 113.54 (C14), 106.09 (C10), 55.57 (CH₃), 40.01 (CH₃), 38.76 (CH), 25.06 (CH₂), 20.43 (CH₃); HR-MS (ESI): m/z calcd for C₂₃H₂₃N₃OS (M + H)⁺, 390.1634; found 390.1639.

4-(4-Nitrophenyl)-5-[1-(6-methoxynaphthalen-2-yl)ethyl]-4H-1,2,4-triazole-3-thione (4f). Orange solid, yield 29%, m.p. 309 °C, R_f 0.80; FT-IR ν_{\max} (cm⁻¹): 3156 (N-H), 3011 (Arom. C-H), 2940 (Aliph. C-H), 1632 (C=N), 1563, 1554, 1505, 1483, 1449 (Arom. C=C, N-H, C-N, N-O), 1266 (C=S), 1212 (C-O). ¹H-NMR (400 MHz, DMSO-*d*₆) δ 1.61 (d, 3H, CH-CH₃), 3.83 (s, 3H, O-CH₃), 5.34 (q, 1H, CH-CH₃), 7.03-7.63 (m, 10H, Ar-H), 8.77 (s, 1H, -NH); ¹³C-NMR (100 MHz, DMSO-*d*₆) δ 175.75 (C=S), 157.55 (C1), 154.12 (C11), 145.85 (C13), 144.22 (C16), 136.91 (C6), 133.49 (C9), 129.39 (C3), 128.59 (C4), 127.53 (C8), 125.98 (C5), 125.80 (C7), 123.60 (C17), 123.12 (C15), 119.11 (C2), 114.85 (C18), 114.81 (C14), 106.12 (C10), 55.09 (CH₃), 37.23 (CH), 20.51 (CH₃); HR-MS (ESI): m/z calcd for C₂₁H₁₈N₄O₃S (M + H)⁺, 407.1172; found 407.1176.

4-(3-Pyridyl)-5-[1-(6-methoxynaphthalen-2-yl)ethyl]-4H-1,2,4-triazole-3-thione (4g). Brown solid, yield 31%, m.p. 122 °C, R_f 0.66; FT-IR ν_{\max} (cm⁻¹): 3153 (N-H), 2964 (Arom. C-H), 2920 (Aliph. C-H), 1635 (C=N), 1566, 1506, 1479, 1432 (Arom. C=C, N-H, C-N), 1266 (C=S), 1226 (C-O). ¹H-NMR (400 MHz, DMSO-*d*₆) δ 1.61 (d, 3H, CH-CH₃), 3.83 (s, 3H, O-CH₃), 4.38 (q, 1H, CH-CH₃), 6.97-7.61 (m, 10H, Ar-H), 8.39 (s, 1H, -NH); ¹³C-NMR (100 MHz, DMSO-*d*₆) δ 175.75 (C=S), 157.52 (C1), 154.40 (C11), 149.55 (C13), 149.07 (C15), 137.11 (C6), 136.58 (C14), 133.45 (C9), 129.43 (C3), 128.60 (C4), 126.41 (C8), 126.01 (C5), 125.68 (C7), 124.22 (C16), 119.18 (C2), 116.45 (C17), 106.12 (C10), 55.57 (CH₃), 37.26 (CH), 20.62 (CH₃); HR-MS (ESI): m/z calcd for C₂₀H₁₈N₄O₃S (M + H)⁺, 363.1274; found 363.1279.

4-Propyl-5-[1-(6-methoxynaphthalen-2-yl)ethyl]-4H-1,2,4-triazole-3-thione (4h). White solid, yield 21%, m.p. 327 °C, R_f 0.82; FT-IR ν_{\max} (cm⁻¹): 3157 (N-H), 2959 (Arom. C-H), 2939 (Aliph. C-H), 1634 (C=N), 1561, 1503, 1484, 1412 (Arom. C=C, N-H, C-N), 1268 (C=S), 12304 (C-O). ¹H-NMR (400 MHz, DMSO-*d*₆) δ 0.59 (t, 3H, CH₂-CH₂-CH₃), 1.47 (m, 2H, CH₂-CH₂-CH₃), 1.59 (d, 3H, CH-CH₃), 2.50 (t, 2H, CH₂-CH₂-CH₃), 3.84 (s, 3H, O-CH₃), 4.37 (q, 1H, CH-CH₃), 7.15-7.79 (m, 6H, Ar-H), 8.43 (s, 1H, -NH); ¹³C-NMR (100 MHz, DMSO-*d*₆) δ 175.67 (C=S), 157.72 (C1), 154.81 (C11), 137.25 (C6), 133.79 (C9), 129.60 (C3), 128.87 (C4), 128.19 (C8), 126.07 (C5), 125.90 (C7), 119.44 (C2), 106.23 (C10), 55.62 (CH₃), 45.00 (CH₂), 36.62 (CH), 24.92 (CH₂), 21.13 (CH₂), 20.84 (CH₃), 11.00 (CH₃); HR-MS (ESI): m/z calcd for C₁₈H₂₁N₃O₃S (M + H)⁺, 328.1478; found 328.1480.

4-Cycloheptylmethyl-5-[1-(6-methoxynaphthalen-2-yl)ethyl]-4H-1,2,4-triazole-3-thione (4i). White solid, yield 47%, m.p. 198 °C, R_f 0.89; FT-IR ν_{\max} (cm⁻¹): 3192 (N-H), 3015 (Arom. C-H), 2925 (Aliph. C-H), 1632 (C=N), 1585, 1506, 1488, 1441 (Arom. C=C, N-H, C-N), 1265 (C=S), 1231 (C-O). ¹H-NMR (400 MHz, DMSO-*d*₆) δ 0.69-1.41 (m, 11H, CH, -CH₂-), 1.59 (d, 3H, CH-CH₃), 2.50 (d, 2H, -CH₂-), 3.84 (s, 3H, O-CH₃), 4.38 (q, 1H, CH-CH₃), 7.15-7.80 (m, 6H, Ar-H), 8.36 (s, 1H, -NH); ¹³C-NMR (100 MHz, DMSO-*d*₆) δ 167.65 (C=S), 157.79 (C1), 154.79 (C11), 137.38 (C6), 133.82 (C9), 129.58 (C3), 128.93 (C4), 128.01 (C8), 126.18 (C5), 125.79 (C7), 119.38 (C2), 106.22 (C10), 55.63 (CH₃), 48.84 (CH₂), 36.72 (CH), 36.65 (C13), 30.40 (C14), 30.17 (C18), 26.09 (C17), 25.61 (C16), 25.52 (C15), 21.74 (CH₃); HR-MS (ESI): m/z calcd for C₂₂H₂₇N₃O₃S (M + H)⁺, 382.1947; found 382.1950.

4-Benzyl-5-[1-(6-methoxynaphthalen-2-yl)ethyl]-4H-1,2,4-triazole-3-thione (4j). White solid, yield 57%, m.p. 296 °C, R_f 0.78; FT-IR ν_{\max} (cm⁻¹): 3200 (N-H), 3010 (Arom. C-H), 2928 (Aliph. C-H), 1632 (C=N), 1557, 1504, 1484, 1453 (Arom. C=C, N-H, C-N), 1257 (C=S), 1225 (C-O). ¹H-NMR (400 MHz, DMSO-*d*₆) δ 1.48 (d, 3H, CH-CH₃), 1.69 (s, 2H, -CH₂-), 3.84 (s, 3H, O-CH₃), 4.64 (q, 1H, CH-CH₃), 7.08-7.71 (m, 11H, Ar-H), 8.51 (s, 1H, -NH); ¹³C-NMR (100 MHz, DMSO-*d*₆) δ 167.86 (C=S), 157.63 (C1), 154.38 (C11), 137.17 (C6), 136.74 (C13), 133.70 (C9), 129.69 (C17), 129.58 (C3), 129.28 (C16), 128.80 (C4), 128.74 (C15), 128.36 (C18), 127.95 (C14), 127.08 (C8), 126.25 (C7), 125.79 (C5), 119.14 (C2), 106.17 (C10), 55.62 (CH₃), 45.99 (CH₂), 37.10 (CH), 21.41 (CH₃); HR-MS (ESI): m/z calcd for C₂₂H₂₇N₃O₃S (M + H)⁺, 376.1478; found 376.1482.

Biological activity

Cell culture and MTT assay. MDA-MB-231 breast cancer cells were cultured and maintained in DMEM containing 10% FBS and supplemented with 1% penicillin/streptomycin. The cultures were incubated at 37 °C in a humidified atmosphere with 5% CO₂. Compounds between 0.1 and 1000 μ M concentration were used for the MTT assay as it is previously reported.⁴⁹ IC₅₀ values were calculated, and cellular analyses were continued with the selected Compound **4b**. Cellular morphological changes were characterized under a microscope.

AO/EB staining. MDA-MB-231 cells were seeded in 12 well plates and reached sufficient confluency. Compound **4b** was added to the wells at IC₅₀ concentration and incubated with the cells for 24 hours. AO/EB dye was prepared, dissolved in PBS at a ratio of 1 : 1, and incubated with the cells for 10 minutes in the dark. Then the cells were washed with PBS, and images were taken under an inverted fluorescence microscope (Zeiss, Axio Vert A1). Green and red dye ratios were analyzed using Image J (NIH, USA).

JC-1 staining. Mitochondrial membrane potential (MMP) was examined using fluorescent dye JC-1 (Abcam, ab113850) as previously described.⁵⁰ MDA-MB-231 cells were seeded in 96 well black plates and reached sufficient confluence. Compound **4b** was added to the wells at IC₅₀ concentration and incubated with the cells for 24 hours. Treated cells were washed with PBS. JC1 solution was added following the instructions and incubated

at 37 °C for 10 minutes and measured at Ex 535 nm, Em 475 nm wavelengths using a fluorescence microplate reader. Red/green fluorescence intensity staining ratios were determined and analyzed.

Caspase-3 activity assay. In order to determine the cell levels of caspase-3 activity,⁵¹ cells were lysed with cell lysis buffer and centrifuged for 10 min at 9000 rpm at 4 °C after treatment with compound 4b for 24 h. Using a commercial kit (Calbiochem, USA) and following the manufacturer's instructions, the supernatant was used for measuring caspase-3 activity as a marker of apoptosis in cells.

Colony formation assay. For the colony formation assay, MDA-MB-231 cells were seeded in 6 well-plates at 400 cells per well. After attachment for 24 h, the cells were treated with doxorubicin (0.006 μM) and **4b** (0.25 μM) in 2 mL of cell culture medium. The cells were left for 14 days of incubation, and the medium was removed. The cells were stained and fixed using 1% crystal violet in 10% methanol for 10 min at room temperature. Afterwards, the crystal violet solution was removed, and the cells were washed with PBS 3 times. More than 50 cells were counted as a colony, and the number of colonies was determined. Images of the colonies were taken using a digital camera. For quantification of colony formation, the cells were destained using 10% acetic acid in dH₂O, and absorbance was measured at 595 nm.

Migration assay. *In vitro* cell invasion was examined by a wound closure assay. MDA-MB231 cells were seeded in 6-well plates at 200 000 cells per well, with three repeats. Cells were left to grow to 95% confluency. The cell monolayer was scratched with a sterile 200 μL pipette tip to create a cross-shaped wound in the middle of each well. A sterile micropipette tip was used at an angle of approximately 90 degrees to keep the width of the scratch constant. The medium in the 6-well plate was removed and the wells were washed with PBS twice to remove the detached cells in the well. 1 μM compound 4b, was added to the wells in the cell culture medium. The total volume of each well was 2 mL. Images were taken on the addition of compound **4b** ($t = 0$ h) and at 12 h and 30 h time intervals. The wound was imaged at 10 times magnification ($t = 0$ h) using a Leica DMi8 live cell microscope equipped with a camera. The obtained images were processed using ImageJ software to calculate the wound area. The wound area after 30 h was normalized to the baseline area at $t = 0$ h.

Cell cycle analyses. Flow cytometry analysis of breast cancer cell cycle phase distributions was performed after treatment with Compound 4b. MDA-MB-231 cells were seeded in 24-well plates at a density of 50 000 cells per well. Following the attachment, the cells were treated with compound **4b** at increasing concentrations from 0.25 μM to 1 μM for 24 h. The cells were trypsinized and collected with centrifugation at 2,000 rpm for 5 min. The cells were fixed using 70% ice-cold ethanol at -20 °C overnight. The ethanol was removed, and the cells were washed with PBS. Then RNase (50 μg mL⁻¹) was added to the cells, and the samples were incubated at 37 °C for 30 min. The cells were collected and stained with propidium iodide (PI) after the RNase treatment. The cells were analyzed

using a flow cytometer (FACS Aria II, BD Biosciences), and the phase distributions were determined according to the DNA content.

Western blot analyses. The Bcl-2 protein level in breast cancer cells after treatment with Compound 4b was determined using Western blotting. MDA-MB-231 cells were seeded in 6 well plates at 150 000 cells per well. After allowing the cells to attach onto the surface, the cells were treated with 0.06 μM doxorubicin and 0.50 μM compound **4b** for 48 h. The cells were collected and washed with PBS, then RIPA buffer was added to the cells and incubated on ice for 30 min to obtain cell lysates. The samples were centrifuged at 11 000 rpm for 10 min, and the cell membrane was removed. Total protein concentration was determined using the Bradford assay. 40 μg of total protein was subjected to 10% SDS-polyacrylamide gel and run at 100 V for 2 h. The proteins were transferred to a PVDF membrane and incubated with an anti-Bcl-2 antibody (Abcam, 59348) at 4 °C overnight. Following the washing steps, the membrane was incubated in anti-rabbit secondary antibody (Abcam 6721) at room temperature for 2 h. The proteins were visualized using the ChemiDoc MP imaging system (Bio-Rad), and the images were analyzed, and band intensities were determined using ImageLab Software. The relative protein levels were normalized to parental control bands.

In vivo study. All experiments in this study were approved by the Erciyes University Local Ethics Committee for Animal Experiments. *In vivo* experiments of this study were performed in the laboratories of Erciyes University Experimental Research and Application Center (DEKAM). Female Balb/C mice (10 weeks, 25 ± 3 g) were selected in this study.

Acute toxicity test. In order to determine the acute systemic toxic effects of compound **4b**, an acute toxicity test was conducted in 15 healthy Balb/C mice according to European Pharmacopoeia. An acute toxicity test defines the potential systemic toxic effect within 24 h after single-dose drug administration. Briefly, mice were divided into four groups as three treatment groups (5 mg kg⁻¹, 10 mg kg⁻¹, 20 mg kg⁻¹) and healthy control mice. The different doses of compound **4b** were administered to the mice, and saline was administered to the healthy control group. 24 h after the single administration, all mice were observed, and each group was evaluated according to the following criteria;

- (1) It is not toxic at the used dose if there is no dead mouse in the group
- (2) It must be repeated if there is one dead mouse in the group
- (3) It is toxic at the used dose if there are at least two dead mice in a group

It was aimed to investigate the potentially toxic effects of compound 4 at the 5, 10, and 20 mg kg⁻¹ doses in this study.⁵²

Induction of ectopic solid EAC tumors

The potential antitumoral effect of compound **4b** was investigated in a well-defined ectopic solid tumor model of compound **4b** in female mice. For this aim, EACs were suspended in saline and intraperitoneally incubated in two mice with a

0.5 mL injection. The intraperitoneal acid fluid was aspirated with a syringe after 5 days of *in vivo* incubation of EACs. The number of EACs was counted with an automated cell counter (Roche Cedex XS, Germany) and diluted with saline to 10×10^6 cells per milliliter. 18 mice were subcutaneously injected with 2×10^6 cells per animal in a 0.2 mL volume of saline. The mice were randomly divided into three groups, namely EACs ($n = 6$), EACs + low dose compound **4b** (5 mg kg^{-1} , $n = 6$), and EACs + high dose compound **4b** (10 mg kg^{-1} , $n = 6$). Tween 20 (5%) was used to disperse compound **4b** in saline, and the treatments were administered in a volume of 0.1 mL/10 g mice. The treatment algorithm was set as a chemotherapy cycle to avoid its potential cumulative systemic toxicity. For this reason, compound **4b** was administrated once every 2 days for 14 days. Mice were anesthetized with ketamine/xylazine combination and tumor tissues were surgically dissected from the mice. Tumor volumes were measured by a saline-filled graduated cylinder as an indicator of antitumoral activity.

Statistical analyses

The statistical analyses for all experiments were done with Graph Pad Prism 8 software. One-way analysis of variance (ANOVA) and Tukey's *post hoc* test were used to compare tumor volumes among groups in the mice. Data were presented as mean \pm standard error of the mean (SEM), and $p < 0.05$ was considered as a value of statistical significance.

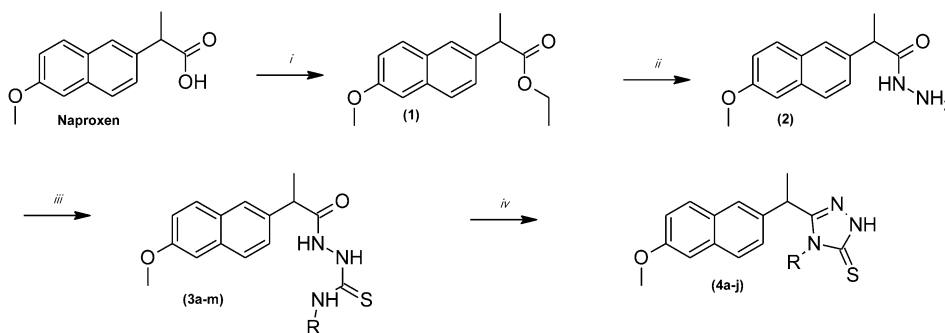
Results and discussion

Chemistry

In this work, we chose (*S*)-Naproxen as a starting compound for the synthesis of new thiosemicarbazide/1,2,4-triazole molecules. In this study, we synthesized twenty-three new compounds, as shown in Scheme 2. In the presence of a few drops of concentrated sulfuric acid (catalyzer), (*S*)-methyl 2-(6-methoxy-2-naphthyl)propanoate (**1**) was synthesized by the reaction of (*S*)-Naproxen and ethanol. Compound **1** and hydrazine hydrate (80%) were refluxed in ethanolic medium, and (*S*)-2-(6-methoxy-2-naphthyl)-propanoic acid hydrazide (**2**) was synthesized (these molecules were synthesized according

to our previous studies).^{41,42} Thiosemicarbazides (**3a-m**) were synthesized with compound **2** and various chosen isothiocyanates in *n*-butanol. 1,2,4-Triazole molecules were synthesized in 4 N NaOH and neutralized using glacial acetic acid from compounds **3a-m**. Compounds **3a-m** and **4a-j** are original molecules. All synthesized compounds were characterized by their melting points, ¹H-NMR, ¹³C-NMR, FT-IR, and HR-MS spectroscopic data.

The results obtained from the spectral data were all compatible with the suggested structures. The FT-IR data showed that hydrazide C=O stretching bands had changed from 1693 cm^{-1} to 1653 cm^{-1} which approved the formation of an amide functionality on the thiosemicarbazides (**3a-m**). Thiosemicarbazide N-H bands were screened at $3194\text{--}3125 \text{ cm}^{-1}$. C=S stretching bands were also detected between $1268\text{--}1253 \text{ cm}^{-1}$, which proved the presence of characteristic thiosemicarbazide C=S stretching bands. The refluxing of (*S*)-Naproxen thiosemicarbazides in aqueous 4 N NaOH changed them into the target compounds (**4a-j**) as indicated in the IR spectra by the appearance of a single absorption for NH in the region $3200\text{--}3128 \text{ cm}^{-1}$. All C=O stretching bands disappeared in the double band region and indicated the formation of triazoles. The absorption bands at $1643\text{--}1632 \text{ cm}^{-1}$ are due to the presence of the C=N stretch of the triazole ring system. Furthermore, the appearance of a C=S absorption band in the region $1268\text{--}1257 \text{ cm}^{-1}$ showed that the triazoles are in their thione form. ¹H-NMR spectra results of N¹, N², and N³ protons (**3a-m**) confirmed the formation of thiosemicarbazide. The thiosemicarbazide protons were taken between 9.15–11.11, 9.33–11.68, and 9.91–12.67 ppm, respectively. All protons were seen according to the expected chemical shifts and integration values in the ¹H-NMR spectra. The ¹H-NMR data of the proposed structures of all synthesized naproxen triazoles were also as expected. Moreover, in the ¹H-NMR spectra of naproxen triazoles (**4a-j**), additional signals due to the NH group appeared in the region of 8.36–8.77 ppm, whereas S-H protons were not detected in the formation of their thionic form. The formation of thiosemicarbazides was also confirmed with ¹³C-NMR studies. The C=O and C=S peaks of compounds **3a-m** were observed between 170.48–176.77 and 177.23–188.13 ppm, respectively. In ¹³C-NMR studies, the compounds (**4a-j**) were



Scheme 2 Synthesized compounds of (*S*)-Naproxen derivatives. (i) $\text{C}_2\text{H}_5\text{OH}/\text{d. H}_2\text{SO}_4$, Δ (ii) $\text{NH}_2\text{NH}_2 \cdot \text{H}_2\text{O}/\text{C}_2\text{H}_5\text{OH}$, Δ (iii) $n\text{-C}_4\text{H}_9\text{OH}/\text{R-NCS}$, Δ (iv) 4 N NaOH/g- CH_3COOH , Δ .

confirmed to be present in thione form with the observation of C=S peaks between 176.22–167.65 ppm. The ^{13}C -NMR spectra of the compounds showed the suitable number of resonances that exactly gathered the number of carbon atoms. HR-MS studies were performed on all thiosemicarbazide and triazole compounds. HR-MS studies confirmed the molecular weights and

empirical formulas within <5 mmu. The molecular ion peaks were observed as expected spots. For all derivatives, the ionization formats were electron spray impact (ESI). All compounds gave the $[M + 1]$ peak at their molecular weight because of catching a hydrogen atom from the medium according to the used method with ESI.

Table 1 IC_{50} results (μM) of the novel (+) (*S*)-Naproxen compounds (**3a–m** and **4a–j**) against MDA-MB-231 cells

Compounds	-R	MDA-MB231	NIH-3T3
3a	$-\text{C}_6\text{H}_4-\text{F}$ (3)	ND	508 ± 12
3b	$-\text{C}_6\text{H}_4-\text{F}_2$ (2,6)	ND	ND
3c	$-\text{C}_6\text{H}_4-\text{Cl}_2$ (2,4)	ND	ND
3d	$-\text{C}_6\text{H}_4-\text{Cl}_2$ (2,6)	ND	269 ± 3
3e	$-\text{C}_6\text{H}_4-\text{Br}$ (2)	845 ± 5	741 ± 6
3f	$-\text{C}_6\text{H}_4-\text{Br}$ (3)	ND	197 ± 1
3g	$-\text{C}_6\text{H}_4-\text{C}_2\text{H}_5$ (4)	ND	479 ± 9
3h	$-\text{C}_6\text{H}_4-\text{NO}_2$ (4)	288 ± 6	163 ± 3
3i	$-\text{C}_5\text{H}_4\text{N}$ (3)	ND	ND
3j	$-\text{C}_3\text{H}_7$	ND	278 ± 6
3k	$-\text{CH}_2-\text{C}_6\text{H}_{11}$	ND	2.69 ± 0.4
3l	$-\text{CH}_2-\text{C}_6\text{H}_5$	ND	396 ± 11
3m	$-\text{CO}-\text{C}_6\text{H}_5$	195 ± 8	ND
4a	$-\text{C}_6\text{H}_4-\text{F}$ (3)	885 ± 14	ND
4b	$-\text{C}_6\text{H}_4-\text{Cl}_2$ (2,4)	9.89 ± 2.4	749 ± 5
4c	$-\text{C}_6\text{H}_4-\text{Cl}_2$ (2,6)	ND	ND
4d	$-\text{C}_6\text{H}_4-\text{Br}$ (3)	ND	ND
4e	$-\text{C}_6\text{H}_4-\text{C}_2\text{H}_5$ (4)	320 ± 7	ND
4f	$-\text{C}_6\text{H}_4-\text{NO}_2$ (4)	778 ± 10	943 ± 14
4g	$-\text{C}_5\text{H}_4\text{N}$ (3)	ND	ND
4h	$-\text{C}_3\text{H}_7$	ND	272 ± 8
4i	$-\text{CH}_2-\text{C}_6\text{H}_{11}$	ND	326 ± 14
4j	$-\text{CH}_2-\text{C}_6\text{H}_5$	ND	8.53 ± 2.02
Doxo		0.06	
Naproxen		> 400	

Biological evaluation

***In vitro* anticancer activity.** The anticancer activity of the synthesized novel naproxen thiosemicarbazide (**3a–m**) and triazole (**4a–j**) molecules was evaluated against the human breast adenocarcinoma cell line ER (–) MDA-MB-231. The NIH-3T3 mouse fibroblast cell line was used for the healthy cell control group. The cytotoxic evaluations were carried out by the 2H-Tetrazolium 2-(4,5-dimethyl-2-thiazolyl)-3,5-diphenyl-bromide (MTT) assay, and subsequently IC_{50} values were acquired.

Among all the compounds, only naproxen triazole compound **4b** demonstrated antitumor activity with IC_{50} value $9.89 \mu\text{M}$ against the MDA-MB-231 breast cancer cell line. Meanwhile, compound **4b** had a higher IC_{50} value ($749 \mu\text{M}$) against the healthy control cell line (NIH-3T3). Only this molecule showed the highest anticancer activity on this cell line. Other molecules did not show any activity. The structures of the Naproxen compounds are dissimilar from each other due to aromatic rings and substituents. Therefore, in these compounds, the presence of 2,4-dichlorophenyl is required for cytotoxic activity. The results of the synthesized compounds are reported in terms of IC_{50} values in Table 1. In order to investigate the potential anticancer activity of the obtained Naproxen triazole compound **4b**, its cytotoxic activity against MDA-MB-231 cells was evaluated with the MTT

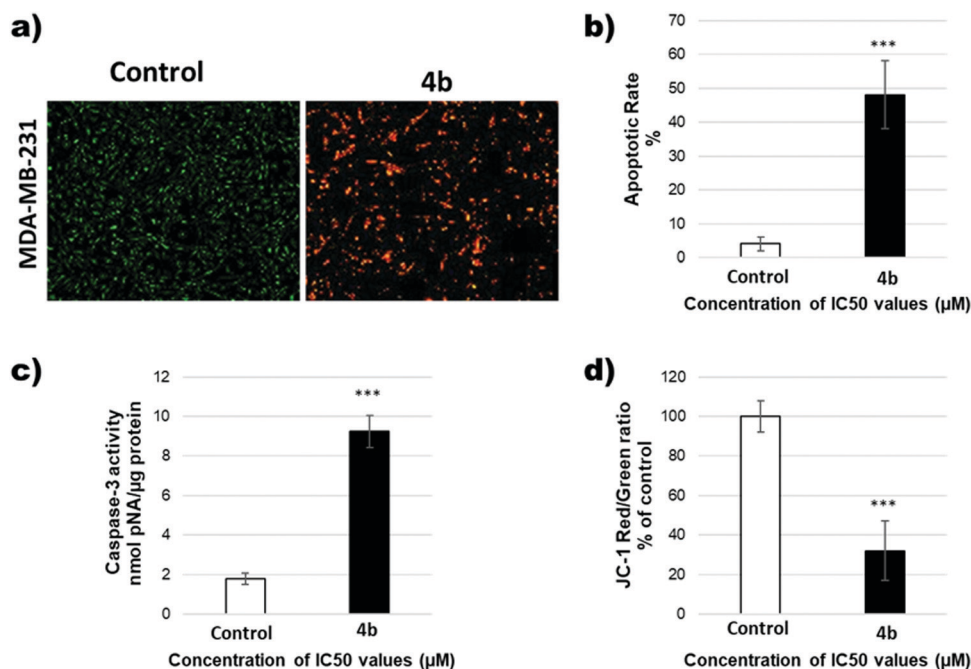


Fig. 1 (a) AO/EB staining of MDA-MB-231 cells treated with compound **4b** for 24 h. (b) Percentage of AO/EB stained cells. (c) Caspase-3 activity of the treated compound **4b** for 24 h in MDA-MB-231 cells. (d) JC-1 staining ratio of the treated compound **4b** for 24 h in MDA-MB-231 cells (*** $p < 0.001$ compared to control).

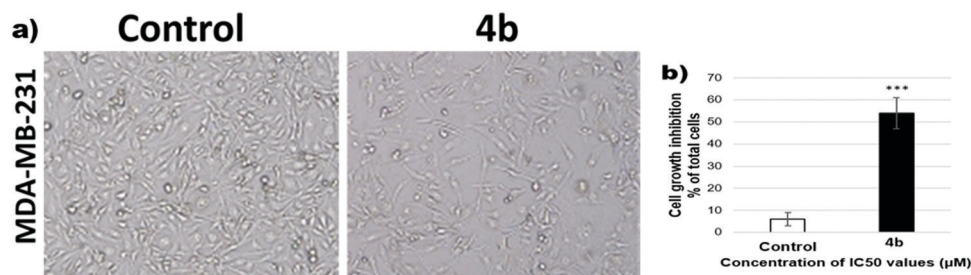


Fig. 2 (a) Cell morphological changes after treatment of compound **4b** in MDA-MB-231 cells for 24 h. (b) Ratio of cell growth in MDA-MB-231 cells treated with compound **4b** for 24 h (***) $p < 0.001$ compared to control).

assay for 24 h. Compound **4b** was bioactive in MDA-MB-231 with IC₅₀ values in micromolar ranges.

AO/EB staining

Fluorescent AO and EB (AO/EB) double staining in MDA-MB-231 cells was used to identify apoptosis-related changes in the cell membranes during the apoptosis process. AO/EB staining of MDA-MB-231 cells showed that live control cells had large green nuclei, indicating that their cell membranes remained intact. However, when treated with Naproxen triazole compound **4b**, the number of cells with large green nuclei was significantly reduced, and almost all cells exhibited nuclear condensation and apoptotic body formation, discoloring orange (Fig. 1). It was observed that apoptotic cells increased significantly with the treatment of Naproxen triazole compound **4b** at the IC₅₀ concentration compared to the untreated control group in MDA-MB-231 (Fig. 2).

JC-1 staining

JC-1 is a special dye used to detect apoptosis in cells due to mitochondrial membrane potential change. The JC-1 dye crosses the cell membrane into the cytosol and moves to the mitochondria. In healthy cells, it remains in the mitochondrial matrix as an aggregate (red); whereas in apoptotic cells, it enters the cytoplasm as a monomer (green) with the disruption of the mitochondrial membrane potential. When MDA-MB-231 cells were incubated with the IC₅₀ concentration of Naproxen triazole compound **4b**, it was observed that JC-1 monomers increased compared to the control group, and the ratio of aggregate to monomer (red/green) in the cells decreased significantly (Fig. 1).

Caspase-3 activity assay

Caspase-3 activity is an important marker in both mitochondrial and extrinsic pathways of apoptosis. When the caspase-3 enzyme is activated, the peptide bonds of many proteins in the cell are cut, and degradation begins and cell death occurs. It was observed that caspase-3 enzyme activity increased significantly in MDA-MB-231 cells treated with Naproxen triazole compound **4b** at the IC₅₀ concentration compared to the control group (Fig. 1).

Colony formation assay

To determine the colony formation ability of single cells treated with compound **4b**, a clonogenic assay was performed. The MDA-MB-231

cells were treated with doxorubicin and compound **4b** and left for 14 days for colony formation. The results (Fig. 3) showed that compound **4b** decreased the colony formation ability of breast cancer cells similar to doxorubicin. The untreated control group had approximately 166 colonies, while the doxorubicin and compound **4b** groups had approximately 80 and 84 colonies, respectively.

Migration assay

We investigated the effect of compound **4b** treatment (1 µM) on cell motility using the wound healing assay. The percentage of wound healing was determined after normalization with DMSO treated cells. The analysis revealed that wound healing was significantly decreased by 64% in MDA-MB-231 cells ($p < 0.001$) at a 1 µM dose of compound **4b** compared to the cells exposed to DMSO (Fig. 4). These results suggest that compound **4b** markedly impairs cell motility of MDA-MB-231 cells.

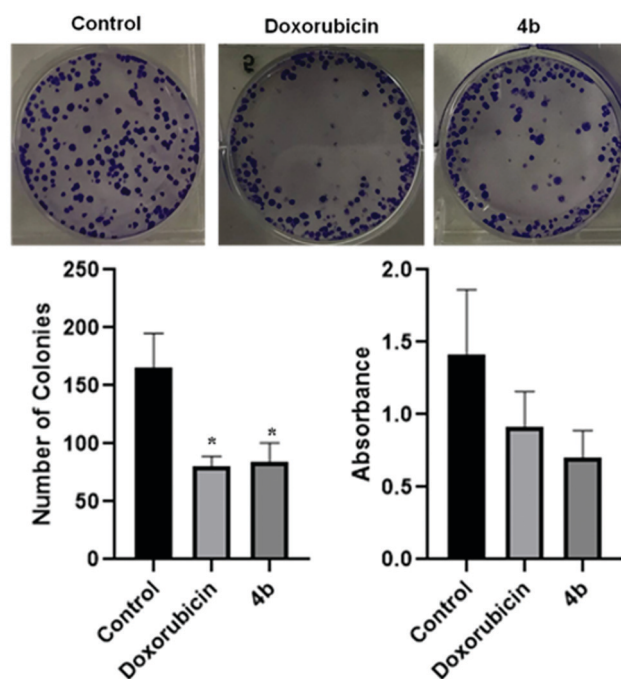


Fig. 3 The effects of doxorubicin and **4b** on colony formation of breast cancer cells.

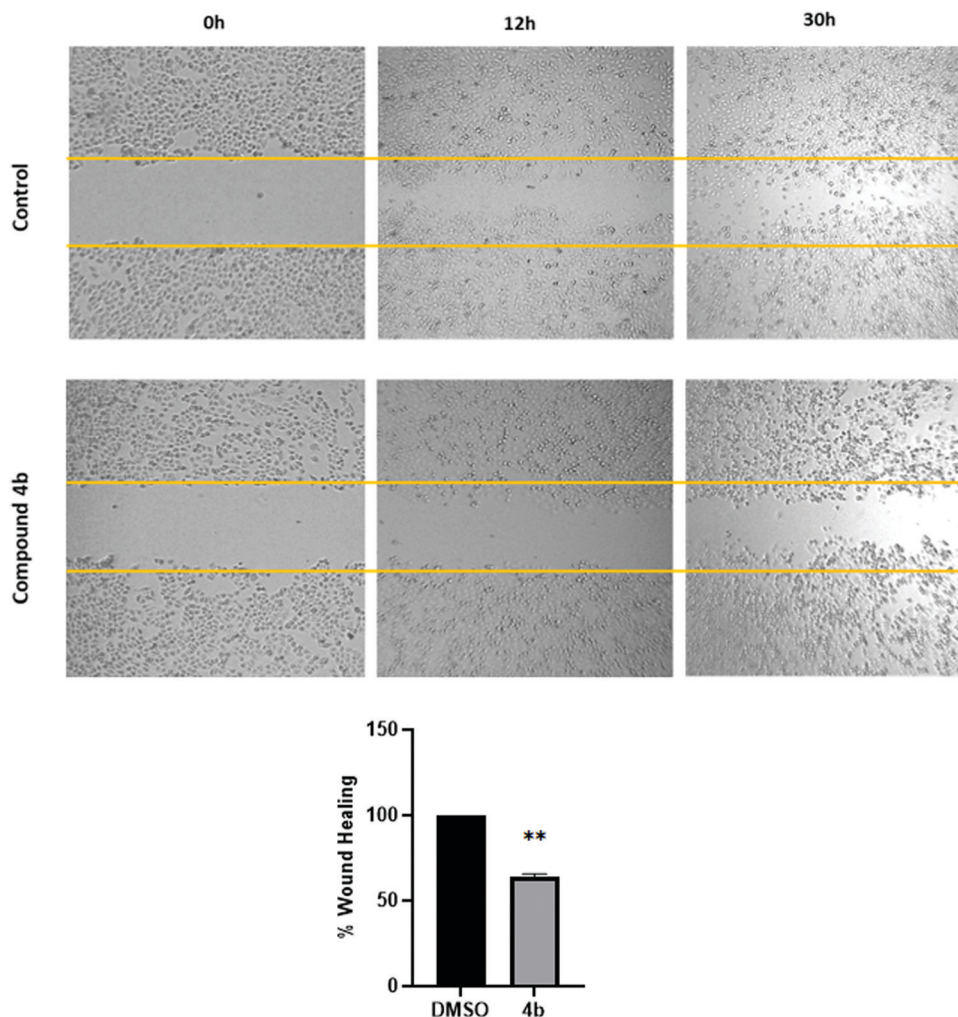


Fig. 4 Compound **4b** inhibits cell migration and invasion in MDA-MB-231 cells. Cell migration was measured by a scratch wound healing assay on MDA-MB-231 cells. The wounded monolayers were treated with $1\ \mu\text{M}$ of compound **4b**. Images were taken at 0, 12 and 30 h after scratching the cultures. Data are represented as mean \pm SD of three independent experiments (** $p < 0.01$ compared to control).

Cell cycle analyses

Anti-cancer drugs cause cellular damage to cancer cells, such as DNA damage, and stimulate cell death. Cancer cell damage inhibits the progression of the cell cycle through checkpoints and causes cell cycle arrest, which induces apoptosis. For the assessment of the anti-cancer activity of compound **4b**, also cell cycle phase distributions of compound **4b**-treated breast cancer cells were evaluated. Fig. 5 shows the effect of compound **4b** on the cell cycle of breast cancer cells. The flow cytometric analysis results showed that compound **4b** decreases the number of cells in the G2/M phase and increases the cells in the S phase in a dose-dependent manner. The percentage of cells in the S phase in the control group was approximately 12, while those for the compound **4b** treated groups at concentrations of 0.25, 0.5, and $1\ \mu\text{M}$ were almost 15, 21, and 28, respectively. The population of control cells in the G2/M phase was approximately 47%, and it decreased to around 18% at $1\ \mu\text{M}$ compound **4b** concentration. The alterations in the cell cycle phase distributions of cancer cells after treatment with compound **4b**

indicate cell cycle arrest and a sign of compound **4b** being a potent anti-cancer drug.

Western blotting

Compound **4b** provided induction of apoptosis in breast cancer cells. Expression of Bcl-2, one of the most overexpressed anti-apoptotic genes in cancer, was determined to evaluate the apoptotic effect of compound **4b** at the molecular level. Fig. 6 shows the level of Bcl-2 protein after treatment with doxorubicin and compound **4b**. It was determined that doxorubicin treatment inhibited Bcl-2 expression by approximately 30%, while compound **4b** suppressed around 60% of Bcl-2 protein expression. The results showed that compound **4b** induced apoptosis through restraining the Bcl-2 protein.

In vivo study

In an acute toxicity test, mice were observed 24 h after the administration of compound **4b** ($5\ \text{mg kg}^{-1}$), compound **4b**

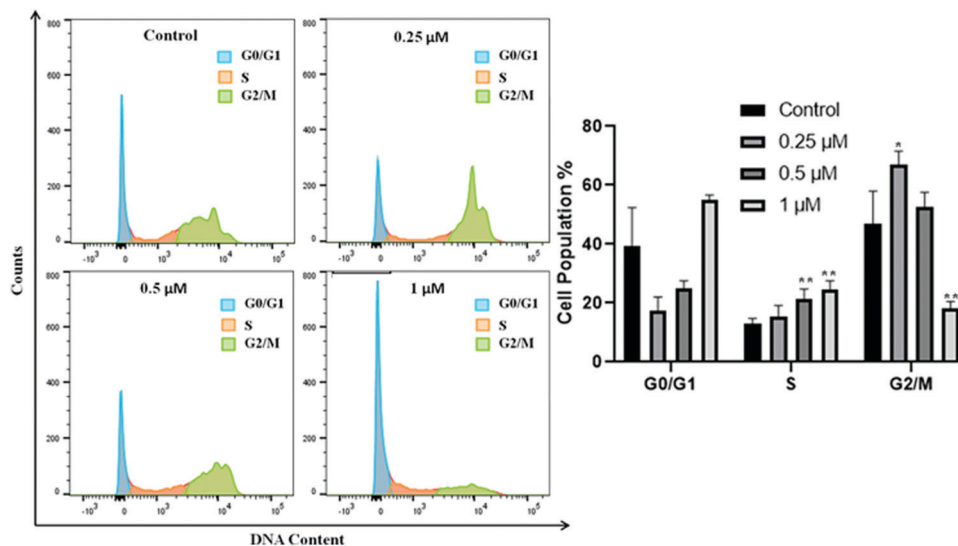


Fig. 5 Cell cycle phase distributions of MDA-MB-231 cells (* $p < 0.05$, ** $p < 0.01$ compared to control).

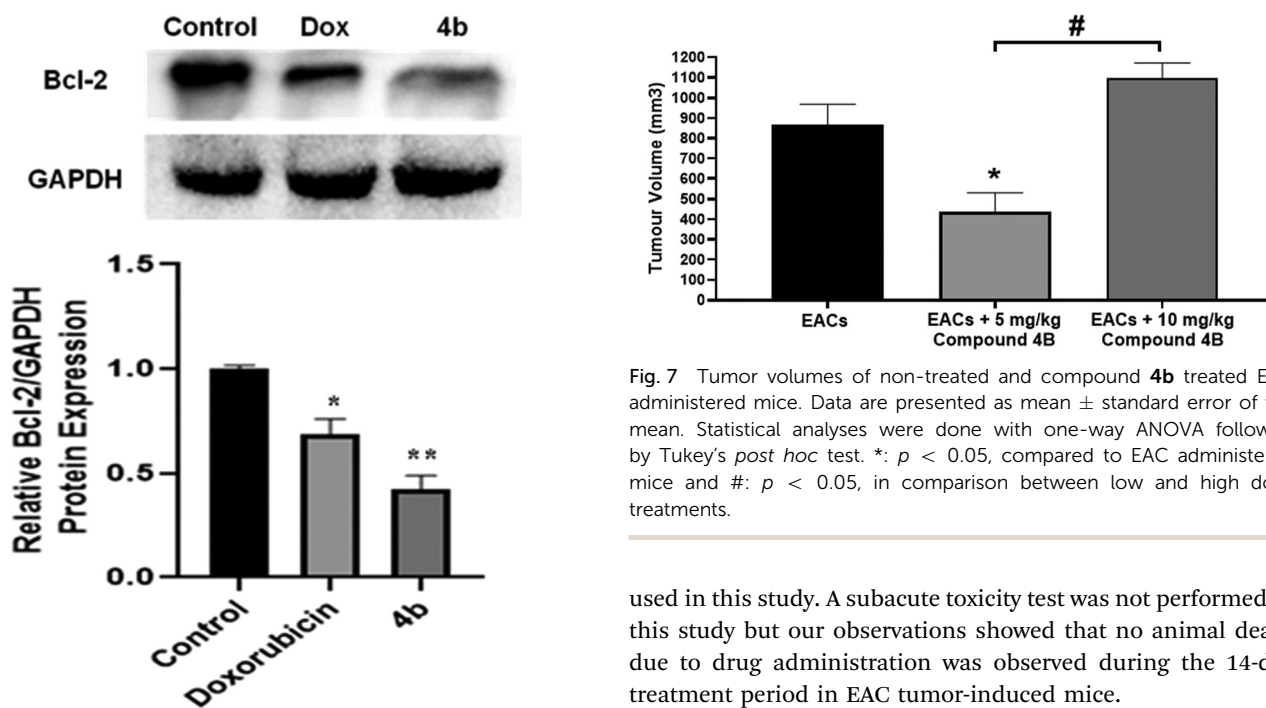


Fig. 6 Expression level of Bcl-2 in MDA-MB-231 cells treated with doxorubicin and compound **4b**.

(10 mg kg⁻¹), or compound **4b** (20 mg kg⁻¹). Three of five animals were dead in the compound **4b** (20 mg kg⁻¹) group. Neither compound **4b** (5 mg kg⁻¹) nor compound **4b** (10 mg kg⁻¹) caused animal death in 24 h following the treatment. Our results showed that compound **4b** is toxic for mice at the dose of 20 mg kg⁻¹, and it was not suitable to use in this study. In addition, it has been shown that compound **4b** did not induce systemic toxicity with a single dose and could be

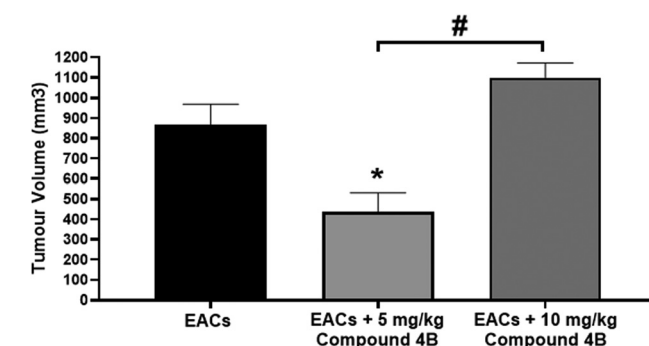


Fig. 7 Tumour volumes of non-treated and compound **4b** treated EAC administered mice. Data are presented as mean \pm standard error of the mean. Statistical analyses were done with one-way ANOVA followed by Tukey's *post hoc* test. *: $p < 0.05$, compared to EAC administered mice and #: $p < 0.05$, in comparison between low and high dose treatments.

used in this study. A subacute toxicity test was not performed in this study but our observations showed that no animal death due to drug administration was observed during the 14-day treatment period in EAC tumor-induced mice.

Tumoral volumes of both treated and non-treated mice were investigated to evaluate the *in vivo* antitumoral activity of compound **4b** in mice. Our results showed that a low dose (5 mg kg⁻¹) of compound **4b** markedly decreased ($p < 0.05$) the tumor volumes compared to the non-treated EAC group. Interestingly, the antitumoral effect of compound **4b** was not maintained at a high dose (10 mg kg⁻¹), and it did not decrease the tumor volumes compared to the EAC group. Furthermore, the tumor volumes of the low dose (5 mg kg⁻¹) compound **4b** treatment were significantly lower than those of the high dose (10 mg kg⁻¹) treatment group (Fig. 7). Representative images of tumor sizes of different groups are presented in Fig. 8.

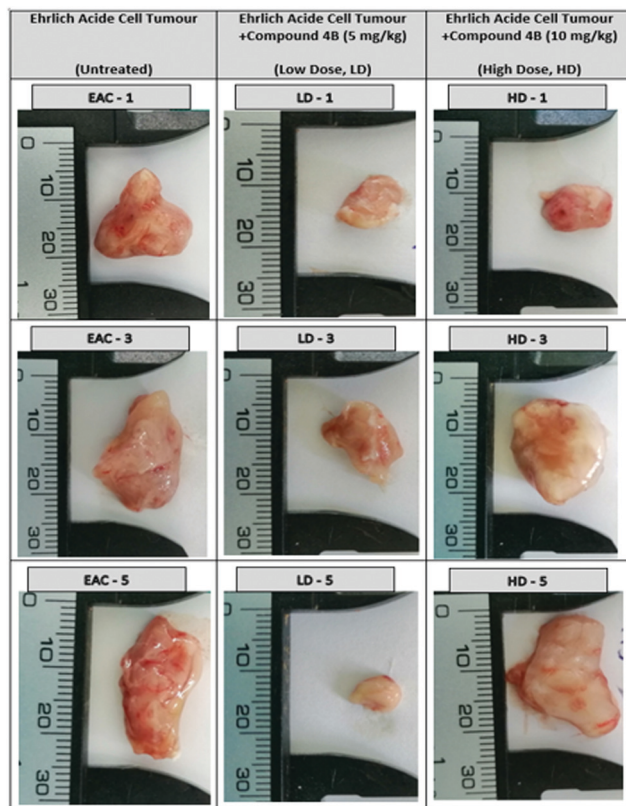


Fig. 8 Representative photographs of the untreated (EACs), low dose and high dose compound **4b** administered mouse tumor tissues.

Conclusion

In conclusion, this study revealed the anticancer activity of thiosemicarbazide and 1,2,4-triazole compounds derived from (*S*)-Naproxen under *in vitro* and *in vivo* conditions. In this study, we synthesized novel molecules and evaluated their anticancer activity against the MDA-MB-231 breast cancer cell line. Among the compounds, (*S*)-4-(2,4-dichlorophenyl)-5-[1-(6-methoxynaphthalen-2-yl)ethyl]-4*H*-1,2,4-triazole-3-thione (**4b**) demonstrated the most potent anticancer activity with a good selectivity ($IC_{50} = 9.89 \pm 2.4$). The *in vitro* cytotoxicity analyses showed that compound **4b** presented an anticancer activity through the Bcl-2 pathway. We controlled the cell cycle analyses, and the results showed that compound **4b** decreases the number of cells in the G2/M phase and increases the cells in the S phase in a dose-dependent manner. Also, the anticancer activity of compound **4b** was evaluated in the Ehrlich acid tumor model, a well-validated *in vivo* ectopic breast cancer model, in mice. Our results showed that compound **4b** has efficient anticancer activity and decreased the tumor volume at both used doses (60 mg kg^{-1} and 120 mg kg^{-1}) in mice because of its potential effects on rapid cell growth.

Author contributions

The manuscript was written through the contributions of all authors. All authors have approved the final version of the

manuscript. These authors contributed equally. M. İhsan Han: investigation, conceptualization, supervision, methodology, resources, writing – original draft, writing – review and editing. Cansu Ümran Tunç: investigation, methodology, visualization, writing – original draft. Pınar Atalay: investigation, methodology, visualization, writing – original draft, writing – review and editing. Ömer Erdoğan: investigation, visualization, writing – original draft. Gökhan Ünal: investigation, visualization, writing – original draft. Mehmet Bozkurt: investigation, writing – original draft. Ömer Aydın: investigation, methodology, visualization, writing – original draft, writing – review & editing. Özge Çevik: investigation, methodology, writing – original draft, writing – review and editing. Ş. Güniz Küçükgül: writing – original draft, writing – review and editing.

Abbreviations

FT-IR	Fourier transform infrared
HR-MS	High-resolution mass spectrometry
NMR	Nuclear magnetic resonance
MTT	(3-(4,5-Dimethyl thiazol-2-yl)-2,5-diphenyltetrazolium bromide) colorimetric method
MDA-MB-231	Human breast cancer cell lines
IC_{50}	50% Inhibition concentration
NSAID	Non-steroidal anti-inflammatory drug
EAC	Ehrlich acid cells
DMSO	Dimethyl sulfoxide
DMEM	Dulbecco's Modified Eagle Media
PBS	Phosphate-buffered saline
LD	Low dose
HD	High dose
ER	Estrogen receptor
EAC	Ehrlich acid tumor

Conflicts of interest

The authors declare that they have no known competing financial interests or personal relationships that could have appeared to influence the work reported in this paper.

Acknowledgements

The authors acknowledge the Research Foundation of Erciyes University (Project Number: THD-2020-10296) for their financial support of this work. "All animal procedures were performed in accordance with the Guidelines for Care and Use of Laboratory Animals of Erciyes University and approved by the Animal Ethics Committee of Local Animal Ethical Committee of Erciyes University (protocol number: 22/042). The starting compound, (*S*)-Naproxen, was obtained from Deva İlaç San. Tic. A. Ş.

References

- 1 R. C. Richie and J. O. Swanson, Breast cancer: A review of the literature, *J. Insur. Med.*, 2003, **35**, 85–101.

- 2 J. L. Kelsey, A review of the epidemiology of human breast cancer, *Epidemiol. Rev.*, 1979, **1**, 74–109.
- 3 B. MacMahon, P. Cole and J. Brown, Etiology of human breast cancer: A review, *J. Nat. Can. Ins*, 1973, **50**, 21–42.
- 4 A. G. Waks and E. P. Winer, Breast cancer treatment a review, *JAMA*, 2019, **321**(3), 288–300.
- 5 R. Ismail-Khan and M. M. Bui, A review of triple-negative breast cancer, *Cancer Control*, 2010, **17**(3), 173–176.
- 6 R. N. Brogden, R. M. Pinder, P. R. Sawyer, T. M. Speight and G. S. Avery, Naproxen: A review of its pharmacological properties and therapeutic efficacy and use, *Drugs*, 1975, **9**, 326–363.
- 7 R. N. Brogden, R. C. Heel, T. M. Speight and G. S. Avery, Naproxen up to date: A review of its pharmacological properties and therapeutic efficacy and use in rheumatic diseases and pain states, *Drugs*, 1979, **18**, 41–277.
- 8 L. Mason, J. E. Edwards, R. A. Moore and H. J. McQuay, Single-dose oral naproxen for acute postoperative pain: A quantitative systematic review, *BMC Anesthesiol.*, 2003, **3**, 1–7.
- 9 M. M. A. Khalifa, M. M. F. Ismail, S. I. Eisa and Y. Ammar, Design and synthesis of some novel 6-methoxynaphthalene derivatives with potential anticancer activity, *Der. Pharm. Chem.*, 2012, **4**(4), 1552–1566.
- 10 T. Aboul-Fadl, S. S. Al-Hamad, K. Lee, N. Li, B. D. Gary, A. B. Keeton, G. A. Piazza and M. K. Abdel-Hamid, Novel non-cyclooxygenase inhibitory derivatives of naproxen for colorectal cancer chemoprevention, *Med. Chem. Res.*, 2014, **23**, 4177–4188.
- 11 J. Deb, J. Majumder, S. Bhattacharyya and S. S. Jana, A novel naproxen derivative capable of displaying anti-cancer and anti-migratory properties against human breast cancer cells, *BMC Cancer*, 2014, **14**, 567–574.
- 12 M. S. Kim, J. E. Kim, D. Y. Lim, Z. Huang, H. Chen, A. Langfald, R. A. Lubet, C. J. Grubbs, Z. Dong and A. M. Bode, Naproxen induces cell-cycle arrest and apoptosis in human urinary bladder cancer cell lines and chemically induced cancers by targeting PI3K, *Cancer Prev. Res.*, 2014, **7**(2), 236–245.
- 13 R. A. Lubet, J. M. Scheiman, A. Bode, J. White, L. Minasian, M. M. Juliana, D. L. Boring, V. E. Steele and C. J. Grubbs, Prevention of chemically induced urinary bladder cancers by Naproxen: Protocols to reduce gastric toxicity in humans do not alter preventive efficacy, *Cancer Prev. Res.*, 2015, **8**(4), 296–302.
- 14 D. Mahendiran, P. Gurumoorthy, K. Gunasekaran, R. S. Kumar and A. K. Rahiman, Structural modeling, *in vitro* antiproliferative activity, and the effect of substituents on the DNA fastening and scission actions of heteroleptic copper(II) complexes with terpyridines and naproxen, *New J. Chem.*, 2015, **39**, 7895–7911.
- 15 D. J. Morre and D. M. Morre, tNOX, an alternative target to COX-2 to explain the anticancer activities of non-steroidal anti-inflammatory drugs (NSAIDs), *Mol. Cell. Biochem.*, 2006, **283**, 159–167.
- 16 T. M. K. Motawi, Y. Bustanji, S. EL-Maraghy, M. O. Taha and M. A. S. Al-Ghusein, Evaluation of naproxen and cromolyn activities against cancer cells viability, proliferation, apoptosis, p53 and gene expression of surviving and caspase-3, *J. Enz. Inhib. Med. Chem.*, 2014, **29**(2), 153–161.
- 17 H. L. Nicastro, C. J. Grubbs, M. M. Juliana, A. M. Bode, M. S. Kim, Y. Lu, M. You, G. L. Milne, D. Boring, V. E. Steele and R. A. Lubet, Preventive effects of NSAIDs, NO-NSAIDs, and NSAIDs Plus difluoromethylornithine in a chemically induced urinary bladder cancer model, *Cancer Prev. Res.*, 2014, **7**(2), 246–254.
- 18 R. Kodela, M. Chattopadhyay and K. Kashfi, Synthesis and biological activity of NOSH-naproxen (AVT-219) and NOSH-sulindac (AVT-18A) as potent anti-inflammatory agents with chemotherapeutic potential, *MedChemComm*, 2013, **4**(11), 1–20.
- 19 S. M. Mahmud, E. L. Franco, D. Turner, R. W. Platt, P. Beck, D. Skarsgard, J. Tonita, C. Sharpe and A. G. Aprikian, Use of non-steroidal anti-inflammatory drugs and prostate cancer risk: A population-based nested case-control study, *PLoS One*, 2011, **6**(1), 1–10.
- 20 M. Chattopadhyay, R. Kodela, P. L. Duvalsaint and K. Kashfi, Gastrointestinal safety, chemotherapeutic potential, and classic pharmacological profile of NOSH-naproxen (AVT-219) a dual NO- and H₂S-releasing hybrid, *Pharma. Res. Per.*, 2016, **4**(2), 1–15.
- 21 S. Srinivas and D. Feldman, A phase II trial of calcitriol and naproxen in recurrent prostate cancer, *Anticancer Res.*, 2009, **29**, 3605–3610.
- 22 V. E. Steele, C. V. Rao, Y. Zhang, J. Patlolla, D. Boring, L. Kopelovich, M. M. Juliana, C. J. Grubbs and R. A. Lubet, Chemopreventive efficacy of naproxen and nitric oxide-naproxen in rodent models of colon, urinary bladder, and mammary cancers, *Cancer Prev. Res.*, 2009, **2**(11), 951–956.
- 23 D. C. Stock, P. A. Groome, D. R. Siemens, S. L. Rohland and Z. Song, Effects of non-selective non-steroidal anti-inflammatory drugs on the aggressiveness of prostate cancer, *Prostate*, 2008, **68**, 1655–1665.
- 24 M. I. Han, P. Atalay, C. Ü. Tunç, G. Ünal, S. Dayan, O. Aydın and S. G. Küçükgülzel, Design and synthesis of novel (S)-Naproxen hydrazide-hydrazones as potent VEGFR-2 inhibitors and their evaluation *in vitro/in vivo* breast cancer models, *Bioorg. Med. Chem.*, 2021, **37**, 116097.
- 25 M. I. Han and Ş. G. Küçükgülzel, Anticancer and antimicrobial activities of Naproxen and Naproxen derivatives, *Mini-Rev. Med. Chem.*, 2020, **20**, 1300–1310.
- 26 Ş. G. Küçükgülzel, S. Rollas, H. Erdeniz, M. Kiraz, A. C. Ekinci and A. Vidin, Synthesis, characterization and pharmacological properties of some 4-arylhydrazono-2-pyrazoline-5-one derivatives obtained from heterocyclic amines, *Eur. J. Med. Chem.*, 2000, **35**, 761–771.
- 27 P. Çıkla, P. Arora, A. Basu, T. T. Talele, N. Kaushik-Basu and Ş. G. Küçükgülzel, Etodolac thiosemicarbazides: A novel class of hepatitis C virus NS5B polymerase inhibitors, *Marmara Pharm. J.*, 2013, **17**, 138–146.
- 28 Y. Dadaş, G. P. Coşkun, Ö. Bingöl-Akpınar, D. Özsavcı and Ş. G. Küçükgülzel, Synthesis and anticancer activity of some novel tolmetin thiosemicarbazides, *Marmara Pharm. J.*, 2015, **19**, 259–267.

- 29 G. P. Coşkun and Ş. G. Küçükgülzel, Macromolecular drug targets in cancer treatment and thiosemicarbazides as anticancer agents, *Anti-Cancer Agents Med. Chem.*, 2016, **16**, 1288–1300.
- 30 G. P. Coskun, T. Djikic, T. B. Hayal, N. Türkel, K. Yelekçi, F. Sahin and S. G. Küçükgülzel, Synthesis, molecular docking and anticancer activity of diflunisal derivatives as cyclooxygenase enzyme inhibitors, *Molecules*, 2018, **23**, 1–19.
- 31 G. P. Coskun, T. Djikic, S. Kalaycı, K. Yelekçi, F. Sahin and S. G. Küçükgülzel, Synthesis, molecular modelling and antibacterial activity against helicobacter pylori of novel diflunisal derivatives as urease enzyme inhibitors, *Lett. Drug Des. Discovery*, 2019, **16**, 392–400.
- 32 H. J. Zhang, Y. Qian, D. D. Zhu, X. G. Yang and H. L. Zhu, Synthesis, molecular modeling and biological evaluation of chalcone thiosemicarbazide derivatives as novel anticancer agents, *Eur. J. Med. Chem.*, 2011, **46**, 4702–4708.
- 33 M. Wujec, E. Kędzierska, E. Kuśmierz, T. Plech, A. Wróbel, A. Paneth, J. Orzelska, S. Fidecka and P. Paneth, Pharmacological and structure–activity relationship evaluation of 4-aryl-1-diphenylacetyl(thio)semicarbazides, *Molecules*, 2014, **19**, 4745–4759.
- 34 G. Cihan-Üstündag, E. Gürsoy, L. Naesens, N. Ulusoy-Güzeldemirci and G. Çapan, Synthesis and antiviral properties of novel indole-based thiosemicarbazides and 4-thiazolidinones, *Bioorg. Med. Chem.*, 2016, **24**, 240–246.
- 35 S. Arora, S. Agarwal and S. Singhal, Anticancer activities of thiosemicarbazides/thiosemicarbazones: A review, *Int. J. Pharm. Pharm. Sci.*, 2014, **6**(9), 34–41.
- 36 Y. Sun, W. Wang, Y. Sun and M. Han, Synthesis and biological evaluation of a novel human stem/progenitor cells proliferation activator: 4-(4-(5-Mercapto-1,3,4-oxadiazol-2-yl)phenyl) thiosemicarbazide (Stemazole), *Eur. J. Med. Chem.*, 2011, **46**, 2930–2936.
- 37 S. G. Küçükgülzel, I. Küçükgülzel, E. Tatar, S. Rollas, F. Sahin, M. Gulluce, E. De Clercq and L. Kabasakal, Synthesis of some novel heterocyclic compounds derived from diflunisal hydrazide as potential anti-infective and anti-inflammatory agents, *Eur. J. Med. Chem.*, 2007, **42**, 893–901.
- 38 P. Cıkla-Suzgun, N. Kaushik-Basu, A. Basu, P. Arora, T. T. Talele, I. Durmaz, R. Cetin-Atalay and S. G. Küçükgülzel, Anti-cancer and anti-hepatitis C virus NS5B polymerase activity of etodolac 1,2,4-triazoles, *J. Enzyme Inhib. Med. Chem.*, 2015, **30**(5), 778–785.
- 39 S. G. Küçükgülzel and P. Cıkla-Süzgün, Recent advances bioactive 1,2,4-triazole-3-thiones, *Eur. J. Med. Chem.*, 2015, **97**, 830–870.
- 40 K. Birgül, Y. Yıldırım, H. Y. Karasulu, E. Karasulu, A. I. Uba, K. Yelekçi, H. Bekçi, A. Cumaoglu, L. Kabasakal, O. Yılmaz and S. G. Küçükgülzel, Synthesis, molecular modeling, *in vivo* study and anticancer activity against prostate cancer of (+)(S)-naproxen derivatives, *Eur. J. Med. Chem.*, 2020, **208**, 112841.
- 41 Ö. Yılmaz, B. Bayer, H. Bekçi, A. I. Uba, A. Cumaoglu, K. Yelekçi and Ş. G. Küçükgülzel, Synthesis, anticancer activity on prostate cancer cell lines and molecular modeling studies of flurbiprofen-thioether derivatives as potential target of MetAP (type II), *Med. Chem.*, 2020, **16**(6), 735–749.
- 42 M. İ. Han, H. Bekçi, A. I. Uba, Y. Yıldırım, E. Karasulu, A. Cumaoglu, H. Y. Karasulu, K. Yelekçi, Ö. Yılmaz and Ş. G. Küçükgülzel, Synthesis. molecular modeling. *In vivo* study. and anticancer activity of 1.2.4-triazole containing hydrazide–hydrazones derived from (S)-naproxen, *Arch. Pharm. Chem. Life Sci.*, 2019, **352**, 1–14, DOI: 10.1002/ardp.201800365.
- 43 M. İ. Han, H. Bekçi, A. Cumaoglu and Ş. G. Küçükgülzel, Synthesis and characterization of 1.2.4-triazole containing hydrazide-hydrazones derived from (S)-Naproxen as anti-cancer agents, *Marmara Pharm. J.*, 2018, **22**(4), 559–569, DOI: 10.12991/jrp.2018.98.
- 44 Y. Zhang, W. Liu, Y. Yang, X. Wang, H. Zhu, L. Bai and X. Qiu, Synthesis, molecular modeling, and biological evaluation of 1,2,4-triazole derivatives containing pyridine as potential anti-tumor agents, *Med. Chem. Res.*, 2013, **22**, 3193–3203.
- 45 Ł. Popiołek, U. Kosikowska, L. Mazur, M. Dobosz and A. Malm, Synthesis and antimicrobial evaluation of some novel 1,2,4-triazole and 1,3,4-thiadiazole derivatives, *Med. Chem. Res.*, 2013, **22**, 3134–3147.
- 46 A. Cansız, M. Koparır and A. Demirdağ, Synthesis of some new 4,5-substituted-4H-1,2,4-triazole-3-thiol derivatives, *Molecules*, 2004, **9**, 204–212.
- 47 A. T. Mavrova, D. Wesselinova, J. A. Tsenov and L. A. Lubenov, Synthesis and antiproliferative activity of some new thieno[2,3-d]pyrimidin-4(3H)-ones containing 1,2,4-triazole and 1,3,4-thiadiazole moiety, *Eur. J. Med. Chem.*, 2014, **86**, 676–683.
- 48 P. M. Wood, L. W. L. Woo, M. P. Thomas, M. F. Mahon, A. Purohit and B. V. L. Potter, Aromatase and dual aromatase-steroid sulfatase inhibitors from the letrozole and vorozole templates, *ChemMedChem*, 2011, **6**, 1423–1438.
- 49 P. E. Goss and K. Strasser, Aromatase inhibitors in the treatment and prevention of breast cancer, *J. Clin. Onc.*, 2001, **19**(3), 881–894.
- 50 O. Cevik, H. Acidereli, A. Turut, S. Yildirim and C. Acilan, Cabazitaxel exhibits more favorable molecular changes compared to other taxanes in androgen-independent prostate cancer cells, *J. Biochem. Mol. Toxicol.*, 2020, **34**.
- 51 O. Erdogan, M. Abbak, G. M. Demirbolat, F. Birtekocak, M. Aksel and S. Pasa, Green synthesis of silver nanoparticles *via* Cynara scolymus leaf extracts: The characterization, anticancer potential with photodynamic therapy in MCF7 cells, *PLoS One*, 2019, **14**(6).
- 52 Abnormal Toxicity, European Pharmacopoeia 7.0, p.162.